Toeplitz non-liquids and Toeplitz braiding

Boxi Li,* Yao Zhou,* and Peng Ye[†]
Guangdong Provincial Key Laboratory of Magnetoelectric Physics and Devices,
State Key Laboratory of Optoelectronic Materials and Technologies,
and School of Physics, Sun Yat-sen University, Guangzhou, 510275, China
(Dated: June 5, 2024)

We study a class of 3D non-liquid states called "Toeplitz non-liquids". These states consist of a stack of 2D twisted \mathbb{Z}_N topologically ordered layers along the z-direction; nearby layers are coupled while keeping translational symmetry along z. The effective field theory is described by infinite Chern-Simons (iCS) theory, with a coefficient matrix called "K-matrix" that is of blocktridiagonal Toeplitz matrix-type. With open boundary conditions (OBC) along the z-direction, certain K-matrices exhibit an exotic phenomenon called "Toeplitz braiding", where the mutual braiding statistical phase between two anyons at opposite boundaries oscillates and remains nonzero in the thermodynamic limit. As a necessary condition, this requires boundary zero modes in the K-matrix spectrum under OBC. A key example is the K-matrix resembling the Hamiltonian of the 1D Su-Schrieffer-Heeger insulator. Since the gauge invariance of Chern-Simons theory guarantees integer quantized entries for K-matrices, no usual global symmetries are needed to protect these zero modes or Toeplitz braiding. In order to obtain the general theory, we categorize K-matrices that support Toeplitz braiding into three types and analyze the conditions for each. We further numerically study the analytical results for all types of K-matrices. For comparison, a trivial case is numerically shown, where the mutual statistical phase angle decays exponentially to zero in the thermodynamic limit.

CONTENTS

I.	Introduction	1
II.	Construction of iCS theory and Toeplitz Braiding A. iCS Description of 3-Dimensional Topological Non-Liquid B. Zero Modes and Toeplitz Braiding	3 4
III.	Sorting K -matrices with Boundary Zero Modes A. General Approach to Sorting K -Matrices with Boundary Zero Modes B. Discussion on $\det B = 0$ Cases C. Discussion on $\det B \neq 0$ Cases	6 7 8
IV.	 Numerical Computation on Toeplitz Braiding A. Numerical Computation on Toeplitz Braiding in Type-I Model B. Numerical Computation on Toeplitz Braiding in Type-II Model C. Numerical Computation on Toeplitz Braiding in Type-III Model D. Numerical Computation on Trivial iCS Theory 	8 8 8 10
V.	Conclusions	10
	Acknowledgments	10
	References	10

A.	Detailed Derivation on Sorting Zero Modes of				
	K-matrices	13			
	1. $\det B = 0$	13			
	2. $\det B \neq 0$	15			

I. INTRODUCTION

Phases beyond the symmetry-breaking paradigm have drawn wide attention in the condensed-matter community. Even in the absence of any symmetry, some phases are intrinsically different from trivial product states, exhibiting long-range entanglement patterns. A celebrated example is intrinsic topological order, which originated from the study of the fractional quantum Hall effect and chiral spin liquid [1, 2]. Over the past decade, significant progress has been made in exploring the interplay between symmetry and quantum entanglement, leading to extensive studies on symmetry-protected topological phases and symmetry-enriched topological orders These examples can be categorized into topologically-ordered liquid phases, meaning they have a well-defined thermodynamic limit and can incorporate trivial product states on additional sites [3].

Recently, research on topologically-ordered non-liquid states has flourished, with notable examples including fracton topological order (FTO) [4–13]. These strongly-correlated systems with long-range entanglement possess point-like excitations with limited mobility. The existence of mobility-restricted excitations distinguishes them from conventional intrinsic topological orders where topological excitations can move freely without additional energy costs. The sensitivity to lattice details in FTO prohibits a conventional continuum limit, setting

^{*} These authors contributed equally to this work.

[†] yepeng5@mail.sysu.edu.cn

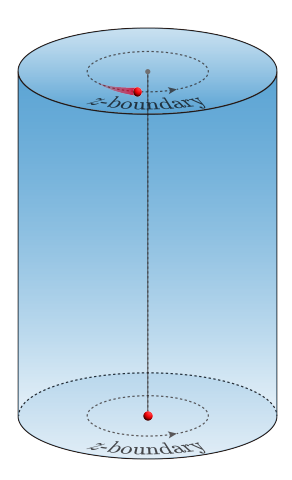


FIG. 1. Illustrative diagram of braiding process between excitations residing at distinct z-boundaries. If the K-matrix of the iCS theory has boundary zero mode, together with the condition that the upper-right and lower-left entries of K^{-1} are non-integers, two topological excitations residing at distinct z-boundaries can be detected mutually via mutual braiding (i.e., Toeplitz braiding) in the thermodynamical limit. Such a type of 3D topologically ordered non-liquids is called "Toeplitz non-liquids" in this paper.

them apart from liquid states [14]. Exactly solvable models like the X-cube model [5] and Haah's code [4] provide insight into these novel properties. Some of these models, including the X-cube model, display a foliation structure, offering insights into some 3+1D¹ FTOs that can be viewed as stacks of coupled 2+1D topological orders. From the entanglement perspective, extracting layers of 2+1D topological orders can be seen as a process of "coarse graining" within the entanglement renormalization group framework. In this context, the Xcube model serves as the fixed point of entanglement renormalization, and the entanglement renormalization group offers a hierarchical structure for a broad range of topologically-ordered non-liquid states [15]. In addition to exactly-solvable lattice models, various field theories [9-11, 16] have been developed to capture the lowenergy physics of topologically-ordered non-liquid states, particularly FTOs. These two different approaches offer complementary perspectives in comprehending the novel properties exhibited by FTOs and other topologicallyordered non-liquid states.

From the analysis of lattice models, it has been observed that certain topologically-ordered non-liquid states can be constructed by stacking topologically-ordered liquid states. This prompts the question of what the field-theoretic counterpart is for the process of stacking topological orders. It is known that the effective theories of 2+1D Abelian topological orders are K-matrix

Chern-Simons theories [17], which provide a framework to understand a large class of topologically-ordered states, including multilayer fractional quantum Hall effects [18], spin liquids [19], and others. They also offer a systematic framework to classify symmetry-enriched topological (SET) and symmetry-protected topological (SPT) phases in 2+1D, see, e.g., Refs. [20–26].

To obtain the stacking physics from the field-theoretic perspective, we start with the Laughlin state, the simplest 2+1D abelian topological order, described by the Chern-Simons theory $\mathcal{L} = \frac{m}{4\pi} a_{\mu} \partial_{\nu} a_{\lambda} \epsilon^{\mu\nu\lambda}$, where a_{μ} is a U(1) gauge field and $m \in \mathbb{Z}$. By stacking the Laughlin states and coupling the nearby layers, we obtain the effective theory for 3-dimensional fractional quantum Hall states. The transport properties of the lateral surfaces of these states have been widely studied both theoretically and experimentally [27–32]. The resulting low-energy effective theory of a 3-dimensional fractional quantum Hall state is a multi-component Chern-Simons (mCS) theory, described by the Lagrangian $\mathcal{L} = \sum_{I=1}^{N} \frac{m}{4\pi} a_{\mu}^{I} \partial_{\nu} a_{\lambda}^{I} \epsilon^{\mu\nu\lambda}$, where N refers to the number of layers. In this context, the index I represents the location of the gauge field in the stacking direction, which is denoted as the z-direction hereafter. If the number of layers is pushed to infinity, the resulting theory is an infinite-component Chern-Simons (iCS) theory.

Very recently, iCS theories have been revisited as effective theories for 3+1D topologically-ordered nonliquid states such as FTOs [14, 33–36]. In fact, the aforementioned 3-dimensional quantum Hall state described by the Lagrangian $\mathcal{L} = \sum_{I=1}^{N} \frac{m}{4\pi} a_{\mu}^{I} \partial_{\nu} a_{\lambda}^{I} \epsilon^{\mu\nu\lambda}$ is a FTO: its ground state degeneracy grows exponentially with the number of layers, and the excitations move only within individual layers. Apart from FTOs, one might ponder other exotic phases that can be captured by the iCS formalism. A more complex iCS theory can be constructed by stacking twisted \mathbb{Z}_m topological orders described by K-matrix Chern-Simons theories $\mathcal{L} = \frac{1}{4\pi} \sum_{I,J} \mathcal{K}_{IJ} a^I_{\mu} \partial_{\nu} a^J_{\lambda} \epsilon^{\mu\nu\lambda}$, where \mathcal{K} is specified as $\mathcal{K} = \begin{pmatrix} n & m \end{pmatrix}$. Here, a^I_{μ} is a U(1) gauge field and n, mare quantized to integers due to the invariance under large-gauge transformations. After stacking these 2+1D twisted topological orders and coupling the nearby lavers by Chern-Simons terms, the K-matrix of the resulting iCS theory is a block-tridiagonal Toeplitz matrix, as shown in Eq. (2). It is crucial to emphasize that the iCS theory we have constructed describes a three-dimensional system, with stacking along the z-direction. Therefore, the superscripts of the gauge fields and the subscripts of the matrix components K_{IJ} in Eq. (1) now correspond to z-coordinates.

Mathematically, Toeplitz matrices are defined as matrices possessing translational symmetry along each diagonal. They find wide applications in both physics and mathematics [37–43]. When the individual entries of a Toeplitz matrix are replaced by matrix blocks, the resulting matrix is referred to as a block Toeplitz matrix. In fact, a block-tridiagonal Toeplitz matrix can be re-

 $^{^1}$ In this paper, "n+1D" refers to n+1-dimensional spacetime, while "nD" refers to n spatial dimensions.

garded as the single-particle Hamiltonian of a 1D tight-binding model. Research on topological insulators (TIs) and topological superconductors (TSCs) has shed light on some Toeplitz matrices possessing eigenvectors localized at boundaries [44–49] when open boundary condition (OPC) is imposed. These eigenvectors have eigenvalues that decrease exponentially to zero as the size of the matrix increases, which is well-known as boundary zero modes. While comparing the Toeplitz K-matrices with Hamiltonians of one-dimensional tight-binding models, it is important to note that the entries in the K-matrix are strictly quantized to integers, and the K-matrix is not the Hamiltonian of the iCS theory.

As is known from the study of TIs and TSCs, boundary zero modes contain rich topological physics. Inspired by research in TIs and TSCs, we wonder whether and how the boundary zero modes of the matrix K reshape the low-lying energy physics of 3+1D topologicallyordered non-liquid states. In this paper, we investigate this question by studying certain iCS theories under OPC in the z-direction (z-OBC). Specifically, we focus on Kmatrices that take the form of block Toeplitz matrices, which possess boundary zero modes. It should be noted that, again, the "boundary zero modes" of K-matrices discussed here are not eigen-energies of topological insulators. Instead, they are eigenvalues of dimensionless K-matrices, which decrease exponentially to zero as the size of the K-matrix, i.e., the number of layers, goes to infinity.

Due to the existence of the boundary zero modes in K-matrix, we find that, the braiding statistics between topological excitations in these iCS theories are highly nonlocal, except for some very special cases where all the upper-right and lower-left components of K^{-1} happen to be integers. In other words, two topological excitations can interact through a braiding process even if they are far apart in the z-direction. For an extreme example, Fig. 1 illustrates the braiding process between topological excitations residing at distinct z-boundaries. Furthermore, we establish the connection that the nonlocal braiding statistics encoded in K^{-1} is a direct consequence of the existence of boundary zero modes in the K-matrix. The braiding phase of two topological excitations residing at distinct z-boundaries is captured by these boundary zero modes and the corresponding small eigenvalues. The mutual braiding statistics induced by boundary zero modes is called "Toeplitz braiding" for keeping track of the nontrivial mathematical properties of Toeplitz matrices. The corresponding 3D bulk state is called "Toeplitz non-liquids".

The paper is organized as follows. In Section II, we carry on an analytic analysis on an iCS theory with Toeplitz braiding, whose K-matrix is, in its mathematical form, equivalent to the Hamiltonian of Su-Schrieffer-Heeger model [44]. In Section III, we propose a general framework for sorting K-matrices with boundary zero modes. Within this framework, we identify three specific types of K-matrices that possess boundary zero modes,

providing them as illustrative examples. The results are shown in Table I. To demonstrate the correspondence between boundary zero modes of K-matrices and nonlocal braiding statistics in z-direction in these models, we conduct numerical computations in Section IV. In Section V, we present the summary and outlook of our study.

II. CONSTRUCTION OF ICS THEORY AND TOEPLITZ BRAIDING

A. iCS Description of 3-Dimensional Topological Non-Liquid

The construction of an iCS theory can be regarded as the process of stacking \mathbb{Z}_m topological order. We initiate our analysis from the \mathbb{Z}_m twisted topological order, which is described by the K-matrix Chern-Simons theory $\mathcal{L} = \frac{1}{4\pi} \sum_{I,J} A_{IJ} a_{\mu}^I \partial_{\nu} a_{\lambda}^J \epsilon^{\mu\nu\lambda}$. Here, A is specified as $A = \begin{pmatrix} n & m \\ 0 & 0 \end{pmatrix}$. Here, a_{μ}^I is a U(1) gauge field and n, m are quantized to integers due to the invariance under large gauge transformations. Given a stack of \mathbb{Z}_m twisted topological order, we add Chern-Simons terms to couple the nearby layers, which corresponds to the upper-right and lower-left blocks in the K-matrix. The stacking direction is dubbed the z-direction hereafter, and the resulting theory is described by the following Lagrangian:

$$\mathcal{L} = \frac{1}{4\pi} \sum_{I,J} K_{IJ} a^I_{\mu} \partial_{\nu} a^J_{\lambda} \epsilon^{\mu\nu\lambda}, \tag{1}$$

where

$$K = \begin{pmatrix} A & B^{T} \\ B & A & B^{T} \\ & B & A & B^{T} \\ & & \ddots & \ddots & \ddots \\ & & & B & A & B^{T} \\ & & & & B & A \end{pmatrix}, \tag{2}$$

with $A=\begin{pmatrix}n&m\\m&0\end{pmatrix}$ and $B=\begin{pmatrix}l_1&l_2\\l_3&l_4\end{pmatrix}$, as shown in Eq. (2). Fig. 2 gives an illustration of the stacking process. If we stack N layers of twisted \mathbb{Z}_m topological order, the resulting theory is a multi-component Chern-Simons (mCS) theory with a 2N-dimensional K-matrix. As the number of layers N goes to infinity, the mCS theory becomes an iCS theory. All the coefficients in the K-matrix are integers due to large gauge invariance. In this setting, the superscript I of a gauge field a^I_μ carries the meaning of the z-coordinate. The I-th layer contains two independent gauge fields a^{2I-1}_μ and a^{2I}_μ . We should be extremely careful about the general basis transformation $K \to W^{\rm T} KW$, $W \in GL(2N,\mathbb{Z})$, requiring it to preserve the locality in the z-direction. The absence of upper-right and lower-left blocks indicates that we are discussing iCS theories in z-OBC.

Sufficient condition for 10cpus ordanis.								
	A	B	Requirements	# of Zero Modes	Boundary Condition			
Type-I	$\begin{pmatrix} n & m \\ m & 0 \end{pmatrix}$	$\begin{pmatrix} l_1 & l_2 \\ l_3 & 0 \end{pmatrix}$	$ m < l_2 + l_3 \ n(l_2 + l_3) = 2l_1 m \ l_2 eq l_3$	2	Both (17a) and (17b)			
Type-II	$\begin{pmatrix} n & m \\ m & 0 \end{pmatrix}$	$\begin{pmatrix} l_1 & l_2 \\ l_3 & 0 \end{pmatrix}$	$ m < l_2 + l_3 \ n(l_2 + l_3) \neq 2l_1 m \ l_2 \neq l_3$	1	$ l_2 < l_3 , (17a)$ $ l_2 > l_3 , (17b)$			
Type-III	$\begin{pmatrix} n & m \\ m & 0 \end{pmatrix}$	$\begin{pmatrix} l_1 & l_2 \\ l_3 & l_4 \end{pmatrix}$	$ m < l_2 - l_3 $ $l_4 \neq 0$ $\det B = l_1 l_4 - l_2 l_3 = 0$ $(2l_2 m - l_4 n)(2l_3 m - l_4 n) = 0$	1	$2l_3 m = l_4 n, (17a)$ $2l_2 m = l_4 n, (17b)$			

TABLE I. A class of K-matrices with boundary zero modes. It should be noted that the "requirement" column is not the sufficient condition for *Toeplitz braiding*.

To discuss the braiding statistics between topological excitations, excitation terms need to be included in the Lagrangian Eq. (1). In K-matrix Chern-Simons theories, topological excitations are labeled by integer vectors $\mathbf{p}=(p^1,p^2,\ldots,p^{2N})^{\mathrm{T}},\mathbf{q}=(q^1,q^2,\ldots,q^{2N})^{\mathrm{T}},\ldots\in\mathbb{Z}^{2N},$ and the excitation terms corresponding to \mathbf{p} and \mathbf{q} are given by $p^Ia^I_\mu j^\mu_{\mathbf{q}}$ and $q^Ia^I_\mu j^\mu_{\mathbf{q}}$, respectively, where $j^\mu_{\mathbf{q}}$ and $j^\mu_{\mathbf{q}}$ are the currents of topological excitations. After integrating out the gauge fields, the mutual braiding phase between topological excitations \mathbf{p} and \mathbf{q} is given by $2\pi p^I(K^{-1})_{IJ}q^J$.

In the following discussion, we use \mathbf{l}_I , $I \in 1, \ldots, 2N$ to label the topological excitation carrying unit gauge charge, coupled to gauge field a_{μ}^{I} . For example, $\mathbf{l}_1 = (1,0,\ldots,0)^{\mathrm{T}}$ labels an excitation coupled to the a_{μ}^{I} gauge field, residing at a z-boundary, while $\mathbf{l}_{2N} = (0,\ldots,0,1)^{\mathrm{T}}$ labels an excitation residing at another z-boundary, coupled to gauge field a_{μ}^{2N} . The mutual braiding phase between \mathbf{l}_1 and \mathbf{l}_{2N} is $2\pi(K^{-1})_{1,2N}$. This example also tells us that the lower-left and upper-right elements of K^{-1} describe the braiding phase between excitations residing at distinct z-boundaries, as illustrated in Fig. 3(a). On the contrary, the diagonal elements of K^{-1} characterize the braiding statistics of excitations in close proximity in the z-direction, as illustrated in Fig. 3(b).

B. Zero Modes and Toeplitz Braiding

In this paper, we focus on Toeplitz braiding in the z-direction induced by the boundary zero modes of the K-matrix of the iCS theory. The zero modes have the following properties: for a finite size K-matrix, the zero modes have finite values instead of being zero. As the size of the system, i.e., the size of the K-matrix, increases, the eigenvalues decrease to zero exponentially. Therefore, for a finite size K-matrix, the inverse K^{-1} is always well-defined. In the following discussion, we mainly focus on the asymptotic behavior of K^{-1} as the number of layers $N \to \infty$. Thus, in the following discussion, the inverse of K is calculated before taking the limit of the system size $2N \to \infty$. To gain insights, we focus on a simple

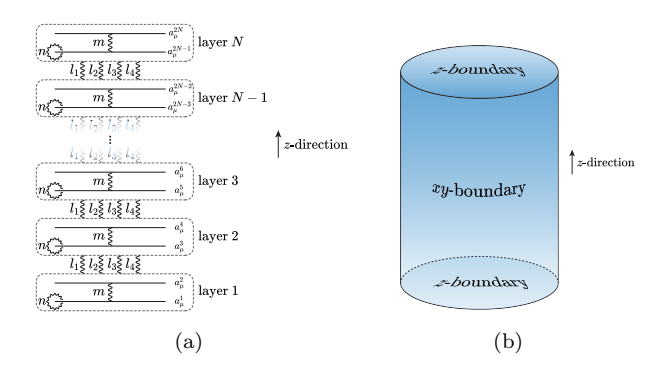


FIG. 2. (a) is an illustrative diagram of stacking \mathbb{Z}_m twisted topological orders. Each layer is a \mathbb{Z}_m twisted topological order described by K-matrix Chern-Simons theory corresponding to diagonal blocks A in the Toeplitz K-matrix. The nearby layers are coupled by Chern-Simons terms, which corresponds to the upper-right and lower-left 2×2 blocks B in the Toeplitz K-matrix. For example, layer 1 contributes intra-layer Chern-Simons terms $\frac{1}{4\pi} [m(a_{\mu}^1 \partial_{\nu} a_{\lambda}^2 + a_{\mu}^2 \partial_{\nu} a_{\lambda}^1) +$ $n(a_{\mu}^{1}\partial_{\nu}a_{\lambda}^{1})]\epsilon^{\mu\nu\lambda}$. The inter-layer Chern-Simons terms between layer 1 and layer 2 are $\frac{1}{4\pi}[l_{1}(a_{\mu}^{1}\partial_{\nu}a_{\lambda}^{3}+a_{\mu}^{3}\partial_{\nu}a_{\lambda}^{1})+l_{2}(a_{\mu}^{3}\partial_{\nu}a_{\lambda}^{2}+a_{\mu}^{3}\partial_{\nu}a_{\lambda}^{2})$ $a_{\mu}^{2}\partial_{\nu}a_{\lambda}^{3}$ + $l_{3}(a_{\mu}^{4}\partial_{\nu}a_{\lambda}^{1} + a_{\mu}^{1}\partial_{\nu}a_{\lambda}^{4}) + l_{4}(a_{\mu}^{4}\partial_{\nu}a_{\lambda}^{2} + a_{\mu}^{2}\partial_{\nu}a_{\lambda}^{4})]\epsilon^{\mu\nu\lambda}$. After stacking these \mathbb{Z}_m twisted topological orders, we obtain a 3-dimensional theory as illustrated in (b). In the following discussion, open boundary condition is applied in z-direction while periodic boundary condition is applied to xy-direction, i.e. each layer of \mathbb{Z}_m twisted topological order is defined on a torus. In our discussion, we focus on the asymptotic behaviour as the number of layer N goes to infinity.

example, where the Lagrangian is given by Eq. (1), and the K-matrix is given by Eq. (2). The A and B blocks read:

$$A = \begin{pmatrix} 0 & m \\ m & 0 \end{pmatrix}, \quad B = \begin{pmatrix} 0 & l \\ 0 & 0 \end{pmatrix}. \tag{3}$$

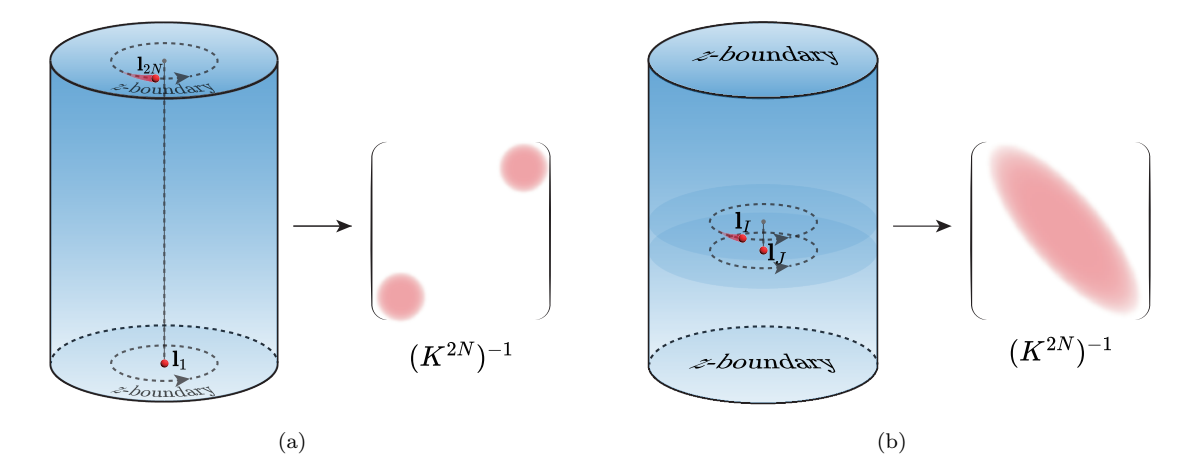


FIG. 3. Fig. (a) is an illustrative diagram of braiding process between topological excitations \mathbf{l}_1 and \mathbf{l}_{2N} locating at distinct z-boundaries. The mutual braiding phase between \mathbf{l}_1 and \mathbf{l}_{2N} is $2\pi[(K^{2N})^{-1}]_{1,2N}$. In general, upper-right and lower-left elements of matrix $(K^{2N})^{-1}$ describe braiding statistics between topological excitations residing at distinct z-boundaries. Fig. (b) is an illustrative diagram of braiding process between topological excitations \mathbf{l}_I and \mathbf{l}_J that are close in z-coordinates $(|I-J| \ll 2N)$. The mutual braiding phase between \mathbf{l}_I and \mathbf{l}_J is $2\pi[(K^{2N})^{-1}]_{IJ}$, which corresponds to the diagonal elements of matrix $(K^{2N})^{-1}$.

Denote the K-matrix of size 2N with block A, B as K_1^{2N} . The inverse $(K_1^{2N})^{-1}$ reads [50]

$$(K_1^{2N})^{-1} = \\ \begin{pmatrix} 0 & \frac{1}{m} & 0 & -\frac{l}{m^2} & 0 & \cdots & 0 & \frac{1}{m} \left(-\frac{l}{m}\right)^{N-1} \\ \frac{1}{m} & 0 & 0 & 0 & 0 & \cdots & 0 & 0 \\ 0 & 0 & 0 & \frac{1}{m} & 0 & \cdots & 0 & \frac{1}{m} \left(-\frac{l}{m}\right)^{N-2} \\ -\frac{l}{m^2} & 0 & \frac{1}{m} & 0 & 0 & \cdots & 0 & 0 \\ \vdots & \vdots & \vdots & \vdots & \vdots & \vdots & \ddots & \vdots & \vdots \\ 0 & 0 & 0 & 0 & 0 & \cdots & 0 & \frac{1}{m} \\ \frac{1}{m} \left(-\frac{l}{m}\right)^{N-1} & 0 & \frac{1}{m} \left(-\frac{l}{m}\right)^{N-2} & 0 & \frac{1}{m} \left(-\frac{l}{m}\right)^{N-3} & \cdots & \frac{1}{m} & 0 \end{pmatrix},$$

which captures the braiding statistics between topological excitations. Following the notation in Section II A, the topological excitation carrying unit gauge charge, coupled to gauge field a_{μ}^{I} , is labelled by

$$\mathbf{l}_I = \begin{pmatrix} \cdots & 0 & 0 & 1 & 0 & 0 & \cdots \end{pmatrix}^T. \tag{5}$$

The subscript I refers to the location of the nonzero component. In the case of |m| > |l|, the mutual braiding phase between \mathbf{l}_I and \mathbf{l}_J is $2\pi[(K_1^{2N})^{-1}]_{IJ}$, decaying exponentially with respect to |I-J|, which means that if two excitations reside at distinct z-boundaries, they cannot "feel" each other by braiding process. For instance, the mutual braiding phase between two excitations $\mathbf{l}_1 = \begin{pmatrix} 1 & 0 & \cdots & 0 \end{pmatrix}^T$ and $\mathbf{l}_{2N} = \begin{pmatrix} 0 & \cdots & 0 & 1 \end{pmatrix}^T$ is $\frac{2\pi}{m} \left(\frac{-l}{m}\right)^N$. Since |l/m| < 1, the braiding phase is oppressed to zero in thermodynamic limit $N \to \infty$. If |l| > |m|, the matrix element $[(K_1^{2N})^{-1}]_{IJ}$ increases exponentially with |I-J| for I, J satisfying I > J, $I \in 2\mathbb{Z}^+$, $J \in 2\mathbb{Z}^+ - 1$ or J > I, $J \in 2\mathbb{Z}^+$, $I \in 2\mathbb{Z}^+ - 1$. The mutual braiding phase $\frac{2\pi}{m} \left(\frac{-l}{m}\right)^N \mod 2\pi$ between \mathbf{l}_1 and \mathbf{l}_{2N} is not exponentially suppressed if $l \mod m^2 \neq 0$, which indicates that topological excitations \mathbf{l}_1 and \mathbf{l}_{2N}

can feel each other in the braiding process. As the system size increases, the braiding phase between two excitations located at distinct z-boundaries, \mathbf{l}_1 and \mathbf{l}_{2N} , exhibits oscillation within the range of 0 to 2π , as shown in Fig. 4.

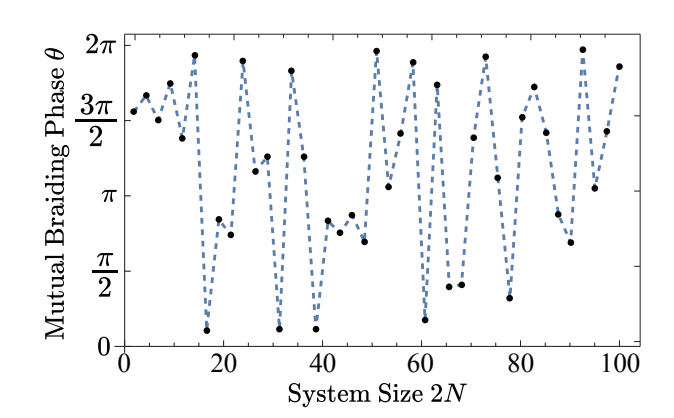


FIG. 4. As the system size 2N increases, the braiding phase $2\pi l_1^T (K_1^{2N})^{-1} l_{2N}$ exhibits oscillations between 0 and 2π . Here we take m=2, l=3.

Furthermore, we will demonstrate that the presence of *Toeplitz braiding* requires boundary zero modes. As is known, if |l| > |m|, the K_1^{2N} matrix has boundary zero modes \mathbf{v}_1 and \mathbf{v}_2 [49],

$$\mathbf{v}_1 = \frac{1}{\sqrt{2}}\psi_1 + \frac{1}{\sqrt{2}}\psi_2,\tag{6}$$

$$\mathbf{v}_2 = -\frac{1}{\sqrt{2}}\psi_1 + \frac{1}{\sqrt{2}}\psi_2,\tag{7}$$

where

$$\psi_{1} = \sqrt{\frac{1 - \left(\frac{m}{l}\right)^{2}}{1 - \left(\frac{m}{l}\right)^{2N}}}, (8)$$

$$\left(1 \ 0 \ \left(-\frac{m}{l}\right) \ 0 \ \left(-\frac{m}{l}\right)^{2} \ \cdots \ \left(-\frac{m}{l}\right)^{N-1} \ 0\right)^{T}$$

$$\psi_{2} = \sqrt{\frac{1 - \left(\frac{m}{l}\right)^{2}}{1 - \left(\frac{m}{l}\right)^{2N}}}$$

$$\left(0 \ \left(-\frac{m}{l}\right)^{N-1} \ 0 \ \left(-\frac{m}{l}\right)^{N-2} \ \cdots \ \left(-\frac{m}{l}\right) \ 0 \ 1\right)^{T}.$$
(9)

Only when the system size $2N \to \infty$, the eigenvalues of boundary zero modes are strictly equal to zero. When the size 2N of matrix K_1^{2N} is finite, the eigenvalues of \mathbf{v}_1 and \mathbf{v}_2 are denoted as λ_1 and λ_2 , respectively.

$$\lambda_1 = |m| \frac{1 - \left(\frac{m}{l}\right)^2}{1 - \left(\frac{m}{l}\right)^{2N}} \left(-\frac{m}{l}\right)^{N-1},\tag{10}$$

$$\lambda_2 = -|m| \frac{1 - \left(\frac{m}{l}\right)^2}{1 - \left(\frac{m}{l}\right)^{2N}} \left(-\frac{m}{l}\right)^{N-1}.$$
 (11)

The inverse of K_1^{2N} can be written as

$$(K_1^{2N})^{-1} = \frac{1}{\lambda_1} \mathbf{v}_1 \mathbf{v}_1^{\dagger} + \frac{1}{\lambda_2} \mathbf{v}_2 \mathbf{v}_2^{\dagger} + \frac{1}{\lambda_3} \mathbf{v}_3 \mathbf{v}_3^{\dagger} + \cdots + \frac{1}{\lambda_{2N}} \mathbf{v}_{2N} \mathbf{v}_{2N}^{\dagger},$$

$$(12)$$

 $\mathbf{v}_3,\ldots,\mathbf{v}_{2N}$ are the other eigenvectors of K_1^{2N} . $\lambda_3,\ldots,\lambda_{2N}$ are the corresponding eigenvalues. As far as $(K_1^{2N})^{-1}$ is concerned, $\frac{1}{\lambda_1}$ and $\frac{1}{\lambda_2}$ are eigenvalues of $(K_1^{2N})^{-1}$ with largest absolute values. In the thermodynamic limit $2N\to\infty,\,\frac{1}{\lambda_1}$ and $\frac{1}{\lambda_2}$ diverge to infinity. We wonder what information is captured in

$$M_1^{2N} := \frac{1}{\lambda_1} \mathbf{v}_1 \mathbf{v}_1^{\dagger} + \frac{1}{\lambda_2} \mathbf{v}_2 \mathbf{v}_2^{\dagger}. \tag{13}$$

The rank of M_1^{2N} is 2, thus it is not invertible. Having \mathbf{v}_1 and \mathbf{v}_2 , we are able to write down the matrix M_1

$$\begin{split} M_1^{2N} &= \frac{1}{\lambda_1} \mathbf{v}_1 \mathbf{v}_1^\dagger + \frac{1}{\lambda_2} \mathbf{v}_2 \mathbf{v}_2^\dagger = \\ \begin{pmatrix} 0 & \frac{1}{m} & 0 & -\frac{l}{m^2} & 0 & \cdots & 0 & \frac{1}{m} \left(-\frac{l}{m}\right)^{N-1} \\ \frac{1}{m} & 0 & -\frac{1}{l} & 0 & \frac{1}{m^2} & \cdots & \frac{1}{m} \left(-\frac{m}{l}\right)^{N-1} & 0 \\ 0 & -\frac{1}{l} & 0 & \frac{1}{m} & 0 & \cdots & 0 & \frac{1}{m} \left(-\frac{l}{m}\right)^{N-2} \\ \vdots & \vdots & \vdots & \vdots & \vdots & \vdots & \ddots & \vdots & \vdots \\ -\frac{l}{m^2} & 0 & \frac{1}{m} & 0 & 0 & \cdots & \frac{1}{m} \left(-\frac{m}{l}\right)^{N-2} & 0 \\ 0 & 0 & \frac{1}{m} \left(-\frac{m}{l}\right)^{N-1} & 0 & 0 & \cdots & \frac{1}{m} \left(-\frac{m}{l}\right)^{N-2} & 0 \\ \frac{1}{m} \left(-\frac{l}{m}\right)^{N-1} & 0 & \frac{1}{m} \left(-\frac{l}{m}\right)^{N-2} & \frac{1}{m} \left(-\frac{l}{m}\right)^{N-3} & \cdots & \frac{1}{m} & 0 \end{pmatrix} \end{split}$$

The upper-right and lower-left entries $(M_1^{2N})_{IJ} = \frac{1}{m} \left(-\frac{m}{l}\right)^{(|I-J|+1)/2}$, $I \in 2\mathbb{Z}^+$, $J \in 2\mathbb{Z}^+ - 1$ are exponentially suppressed. Therefore, M_1^{2N} gives good approximation to the upper-right and lower-left elements of

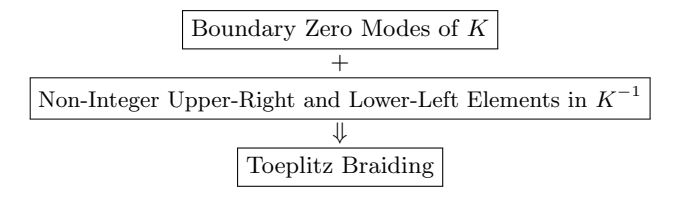


FIG. 5. The condition for Toeplitz braiding.

 $(K_1^{2N})^{-1}.$ In other words, M_1^{2N} captures the long-range braiding statistics in z-direction.

It is noteworthy that in some cases, the nonzero upperright and lower-left elements may not result in truly long-ranged braiding statistics in the z-direction. For example, if $l \mod m^2 = 0$, the upper-right and lowerleft entries in Eq. (4) are integers, implying that the braiding statistics between excitations residing at distinct z-boundaries cannot interact. Indeed, the presence of boundary zero modes is a necessary but not sufficient condition for the appearance of Toeplitz braiding. We have demonstrated that the appearance of boundary zero modes in K-matrices will result in non-zero entries in the upper-right and lower-left regions of K^{-1} . However, the entries in these regions are not guaranteed to be nonintegers. The presence of non-integers in the upper-right and lower-left regions of K^{-1} is necessary for the occurrence of Toeplitz braiding. Therefore, we propose the following condition for the existence of Toeplitz braiding: If boundary zero modes of K along with non-integer upperright and lower-left regions of K^{-1} exist, then Toeplitz braiding occurs., which is also illustrated in Fig. 5.

III. SORTING K-MATRICES WITH BOUNDARY ZERO MODES

A. General Approach to Sorting K-Matrices with Boundary Zero Modes

We have studied an example of iCS theories with Toeplitz braiding. Our investigation into a concrete example of iCS theories with Toeplitz braiding has raised an intriguing question: how to identify and classify iCS theories with Toeplitz braiding? To address this question, we present a systematic framework for determining the presence of boundary zero modes in a given Kmatrix. As shown in Table I, we identify three different types of K-matrices with boundary zero modes as illustrative examples. The K-matrix of Type-I iCS theory exhibits two linearly independent boundary zero modes, whereas the K-matrix of Type-II or Type-III iCS theory possesses only one boundary zero mode. The aforementioned example, an iCS theory with an Su-Schrieffer-Heeger (SSH)-type K-matrix, represents a typical Type-I iCS theory.

Denote the entries of an eigenvector satisfying the

eigenequation $K\psi = \lambda \psi$ as

$$\boldsymbol{\psi} = \begin{pmatrix} \psi_1^A & \psi_1^B & \psi_2^A & \psi_2^B & \cdots & \psi_N^A & \psi_N^B \end{pmatrix}^{\mathrm{T}}.$$
 (15)

In order to determine whether the boundary zero modes exist, the $\lambda \to 0$ limit is taken at first. Under this condition, the entries of ψ are required to satisfy the recurrence relation

$$B\begin{pmatrix} \psi_{j-1}^A \\ \psi_{j-1}^B \end{pmatrix} + A\begin{pmatrix} \psi_j^A \\ \psi_j^B \end{pmatrix} + B^{\mathrm{T}}\begin{pmatrix} \psi_{j+1}^A \\ \psi_{j+1}^B \end{pmatrix} = 0 \tag{16}$$

for $j=2,\ldots,N-1$. Moreover, ψ needs to satisfy the "boundary condition"

$$A \begin{pmatrix} \psi_1^A \\ \psi_1^B \end{pmatrix} + B^{\mathrm{T}} \begin{pmatrix} \psi_2^A \\ \psi_2^B \end{pmatrix} = 0, \tag{17a}$$

$$B\begin{pmatrix} \psi_{N-1}^A \\ \psi_{N-1}^B \end{pmatrix} + A\begin{pmatrix} \psi_N^A \\ \psi_N^B \end{pmatrix} = 0. \tag{17b}$$

To solve the recurrence relation Eq. (20) as well as the "boundary condition" Eq. (17a) and Eq. (17b), we take the following ansatz

$$\psi = \sum_{j} w_{j} \phi^{j}, \tag{18}$$

where $\{w_j\}$ are undetermined coefficients and ϕ^j is assumed to be

$$\phi^{j} = (\phi^{j,A} \ \phi^{j,B} \ \beta_{j}^{2}\phi^{j,A} \ \beta_{j}^{2}\phi^{j,B} \ \cdots \ \beta_{j}^{N-1}\phi^{j,A} \ \beta_{j}^{N-1}\phi^{j,B})^{\mathrm{T}},$$
(19)

It is assumed that ψ is a boundary zero mode localized at one z-boundary, i.e. all the β_j in ϕ^j either satisfies $|\beta_j| > 1$ or $|\beta_j| < 1$. In other words, a potential boundary zero mode ψ can be expressed as a linear combination of vectors in the form Eq. (19), which localizes at one z-boundary. The recurrence relation Eq. (20) gives the equation for $(\phi^{j,A} \phi^{j,B})^{\mathrm{T}}$.

$$B\begin{pmatrix} \phi^{j,A} \\ \phi^{j,B} \end{pmatrix} + \beta_j A \begin{pmatrix} \phi^{j,A} \\ \phi^{j,B} \end{pmatrix} + \beta_j^2 B^{\mathrm{T}} \begin{pmatrix} \phi^{j,A} \\ \phi^{j,B} \end{pmatrix} = 0 \quad (20)$$

Nontrivial solution to $(\phi^{j,A} \phi^{j,B})^{\mathrm{T}}$ gives the equation for β_j

$$\det(B + A\beta_j + B^{\mathrm{T}}\beta_j^2) = 0. \tag{21}$$

Therefore, $\{\beta_i\}$ are the solutions of the equation

$$a + b\beta + c\beta^2 + b\beta^3 + a\beta^4 = 0,$$
 (22)

$$\begin{cases}
 a = l_1 l_4 - l_2 l_3, \\
 b = -(m(l_2 + l_3) - n l_4), \\
 c = -(l_2^2 + l_3^2 - 2 l_1 l_4 + m^2).
\end{cases}$$
(23)

Following this framework, we can systematically determine whether a given K-matrix possesses a boundary zero mode.

It is important to note that if a K-matrix possesses two boundary zero modes, ψ^1 and ψ^2 , satisfying distinct boundary conditions Eq. (17a) and Eq. (17b), respectively, the actual boundary mode for a finite-size Kmatrix is a linear combination of ψ^1 and ψ^2 , which can be obtained by diagonalizing the effective K-matrix

$$\begin{pmatrix} (\boldsymbol{\psi}^1)^{\dagger} K \boldsymbol{\psi}^1 & (\boldsymbol{\psi}^1)^{\dagger} K \boldsymbol{\psi}^2 \\ (\boldsymbol{\psi}^2)^{\dagger} K \boldsymbol{\psi}^1 & (\boldsymbol{\psi}^2)^{\dagger} K \boldsymbol{\psi}^2 \end{pmatrix}. \tag{24}$$

In the subsequent subsections, we provide a detailed discussion on sorting the Type-I, Type-II, and Type-III K-matrices. We organize our analysis based on whether the determinant of matrix B is equal to zero or not. The value of det B plays a crucial role in determining the order of Eq. (22), which affects the # of trial solutions.

B. Discussion on $\det B = 0$ Cases

If det B=a=0, Eq. (22) has a solution $\beta_0=0$, which is discarded. The other two solutions β_1 and β_2 , are determined by the equation

$$b + c\beta_{1,2} + b\beta_{1,2}^2 = 0, (25)$$

from which we know that $\beta_1\beta_2=1$. For the sake of convenience, we set $|\beta_1|<1$, $|\beta_2|>1$. Eq. (20) together with normalization condition gives the solution to $(\phi^{j,A} \phi^{j,B})^{\mathrm{T}}$, j=1,2. If $\psi^1=\phi^1$ is a legitimate boundary zero mode, it needs to satisfy the boundary condition Eq. (17a). Detailed calculation in Appendix A 1 shows that there exists one boundary mode satisfying the boundary condition Eq. (17a) if

$$\begin{cases}
 m \neq 0, & l_4 \neq 0 \\
 |m| < |l_3 - l_2| \\
 l_1 l_4 = l_2 l_3 \\
 2 l_3 m = l_4 n
\end{cases}$$
(26)

Likewise, there exists boundary zero mode $\psi^2 = \phi^2$ satisfying boundary condition Eq. (17b) if

$$\begin{cases}
 m \neq 0, & l_4 \neq 0 \\
 |m| < |l_3 - l_2| \\
 l_1 l_4 = l_2 l_3 \\
 2 l_2 m = l_4 n
\end{cases} ,$$
(27)

The above discussion has ignored $l_4=0$. If $l_4=0$, $a=\det B=0$ enforces $l_2=l_4=0$ or $l_3=0$. If $l_2=0$, $m\neq 0,\ l_3\neq 0,\ n^2+l_1^2\neq 0$, i.e.

$$A = \begin{pmatrix} n & m \\ m & 0 \end{pmatrix}, \quad B = \begin{pmatrix} l_1 & 0 \\ l_3 & 0 \end{pmatrix}, \tag{28}$$

detailed derivation in Appendix A shows that there is one boundary zero mode satisfying boundary condition Eq. (17a) if $|m| < |l_3|$. If $n = l_1 = l_2 = l_4 = 0$, $|m| < |l_3|$, there exists two boundary zero modes.

Similarly, if $l_3 = l_4 = 0$, $m \neq 0$, $l_2 \neq 0$, $n^2 + l_1^2 \neq 0$, i.e.

$$A = \begin{pmatrix} n & m \\ m & 0 \end{pmatrix}, \quad B = \begin{pmatrix} l_1 & l_2 \\ 0 & 0 \end{pmatrix}, \tag{29}$$

there is one boundary zero mode satisfying boundary condition Eq. (17b) if $|m| < |l_2|$. If $n = l_1 = l_3 = l_4 = 0$, $|m| < |l_2|$, the A and B blocks are given by Eq. (3), which has been studied in Section II B.

C. Discussion on $\det B \neq 0$ Cases

If $a \neq 0$, Eq. (22) is a fourth-degree equation. It has 4 solutions β_1 , β_2 , β_3 , β_4 , satisfying $\beta_1\beta_2\beta_3\beta_4 = 1$. Two solutions β_1 , β_2 satisfies $|\beta_1| < 1$, $|\beta_2| < 1$ while the other two satisfies $|\beta_3| > 1$, $|\beta_4| > 1$. Therefore, a legitimate boundary zero mode satisfying boundary condition Eq. (17a) is a linear combination of ϕ^1 and ϕ^2 . Likewise, a legitimate boundary zero mode satisfying boundary condition (17b) is a linear combination of ϕ^3 and ϕ^4 . In general, analyzing the fourth-order equation Eq. (22) can be challenging. It often requires a case-by-case study to determine whether a given K-matrix possesses a boundary zero mode. However, if $l_4 = 0$, Eq. (22) can be factorized into the product of two quadratic polynomials,

$$(l_2 + m\beta + l_3\beta^2)(l_3 + m\beta + l_2\beta^2) = 0,$$
 (30)

which enables a thorough discussion. Detailed analysis are shown in Appendix A 2. We discover that if $l_4 = 0$,

$$\begin{cases} |m| < |l_2 + l_3| \\ n(l_2 + l_3) \neq 2l_1 m \\ l_2 \neq l_3 \end{cases}$$
 (31)

the K-matrix possesses one boundary zero mode. If $l_4 = 0$,

$$\begin{cases} |m| < |l_2 + l_3| \\ n(l_2 + l_3) = 2l_1 m \\ l_2 \neq l_3 \end{cases}$$
 (32)

the K-matrix possesses two boundary zero modes.

As shown in Table I, we find 3 types of K-matrices possessing boundary zero modes. The K-matrix of Type-I iCS theory has 2 boundary zero modes, while K-matrix of Type-II or Type-III iCS theory has only 1 boundary zero mode. We're going to study one example of each type numerically in the upcoming section.

IV. NUMERICAL COMPUTATION ON TOEPLITZ BRAIDING

In order to demonstrate the nonlocal braiding statistics along the z-direction in the presence of boundary zero modes of the K-matrix of iCS theories, we conduct a numerical computation that illustrates the connection

between the appearance of nonlocal braiding statistics and the existence of boundary zero modes. For comparative analysis, we focus on iCS theories that arise from stacking \mathbb{Z}_2 twisted topological orders. The block A in the K-matrix, given by (2), is $\begin{pmatrix} 2 & 2 \\ 2 & 0 \end{pmatrix}$.

A. Numerical Computation on Toeplitz Braiding in Type-I Model

To demonstrate the correspondence between boundary zero modes and Toeplitz braiding in Type-I models, we consider the K-matrix of size 2N given by Eq. (2) with

$$A = \begin{pmatrix} 2 & 2 \\ 2 & 0 \end{pmatrix}, \quad B = \begin{pmatrix} 2 & 1 \\ 3 & 0 \end{pmatrix}. \tag{33}$$

as an example. We denote the K-matrix with blocks A and B given by Eq. (33) as K_2^{2N} , where 2N refers to the size of the K-matrix. As shown in Fig. 6(a1), the braiding phase $2\pi \mathbf{l}_2^{\mathrm{T}}(K_2^{2N})^{-1}\mathbf{l}_{2N}$ between topological excitations residing at distinct z-boundaries oscillates between 0 and 2π as the system size 2N increases, indicating the existence of Toeplitz braiding. This existence can be directly observed from the inverse of K_2^{2N} . The matrix plot of the inverse is shown in Fig. 6(b1), where we consider a system size of 2N=200. K_2^{2N} possesses two boundary zero modes, $\mathbf{v}_{2,1}$ and $\mathbf{v}_{2,2}$. We introduce a matrix constructed by these boundary zero modes:

$$M_2^{2N} = \frac{1}{\lambda_{2,1}} \mathbf{v}_{2,1} \mathbf{v}_{2,1}^{\dagger} + \frac{1}{\lambda_{2,2}} \mathbf{v}_{2,2} \mathbf{v}_{2,2}^{\dagger}.$$
 (34)

Compared to the inverse of the K_2^{2N} -matrix, M_2^{2N} provides a good approximation to the upper-right and lower-left entries of K_2^{2N} , as depicted in Fig. 6(c1), where we define a matrix $(E_2^{2N})_{IJ} = |(M_2^{2N})_{IJ} - (K_2^{2N})_{IJ}^{-1}|$ to characterize the similarity. As the system size 2N increases, the upper-right and lower-left entries of M_2^{2N} and $(K_2^{2N})^{-1}$ converge towards each other, as shown in Fig. 6(d1), where we focus on the asymptotic behavior of $(E_2^{2N})_{2N,2}$ as an example. This observation suggests that we can extract information about the braiding statistics of excitations residing at distinct z-boundaries by analyzing the zero modes and their close-to-zero eigenvalues.

B. Numerical Computation on Toeplitz Braiding in Type-II Model

Likewise, to demonstrate the correspondence between boundary zero modes and Toeplitz braiding in Type-II models, we consider the K-matrix of size 2N given by Eq. (2) with

$$A = \begin{pmatrix} 2 & 2 \\ 2 & 0 \end{pmatrix}, \quad B = \begin{pmatrix} 2 & 4 \\ 2 & 0 \end{pmatrix}. \tag{35}$$

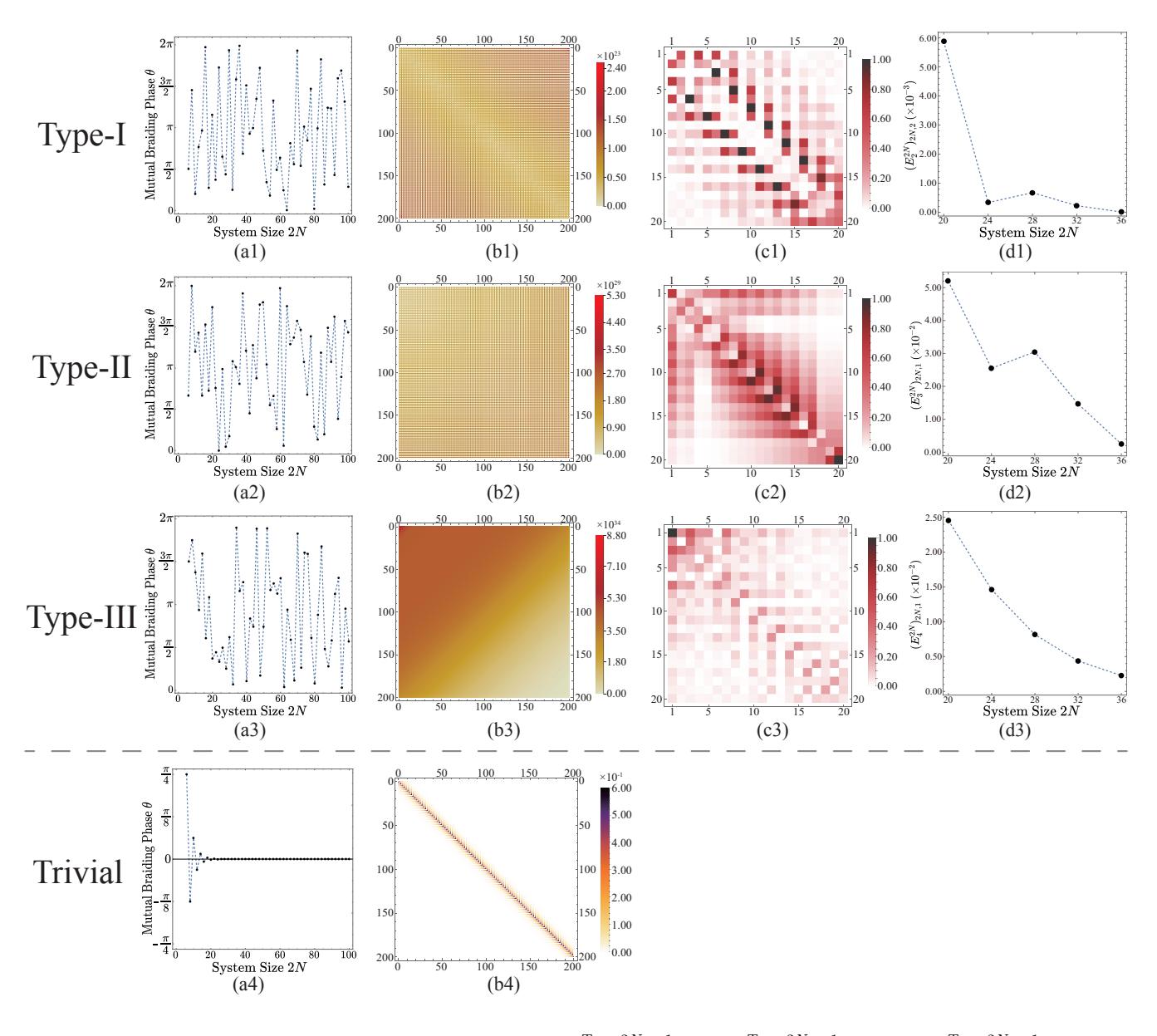


FIG. 6. (a1-a3) respectively show that the braiding phase $2\pi l_1^T(K_2^{2N})^{-1}l_{2N}$, $2\pi l_1^T(K_3^{2N})^{-1}l_{2N}$ and $2\pi l_1^T(K_4^{2N})^{-1}l_{2N}$ exhibit oscillations between 0 and 2π as the system size 2N increases. (b1-b3) are the matrix plots of $(K_2^{2N})^{-1}$, $(K_3^{2N})^{-1}$ and $(K_4^{2N})^{-1}$, respectively, where we set the matrix size to be 2N=200. (c1-c3) are the matrix plots of E_2^{2N} , E_3^{2N} and E_4^{2N} , respectively, where we take the size of the matrix E_2^{2N} to be 20. The matrices E_2^{2N} , E_3^{2N} and E_2^{2N} provide good approximation to the upper-right and lower-left elements of $(K_2^{2N})^{-1}$, $(K_3^{2N})^{-1}$ and $(K_4^{2N})^{-1}$, respectively. This implies that we can extract the braiding statistics of excitations residing at distinct boundaries from the boundary zero modes. (d1-d3) show the lower-left entries $(E_2^{2N})_{2N,2}$, $(E_3^{2N})_{2N,1}$, $(E_4^{2N})_{2N,1}$ of matrix E_2^{2N} , E_3^{2N} , respectively, where we define $(E_{2,3,4}^{2N})_{1J} = |(M_{2,3,4}^{2N})_{1J} - (K_{2,3,4}^{2N})_{1J}|$. As is shown, the lower-left entries of E_2^{2N} , E_3^{2N} , respectively, where we define $(E_{2,3,4}^{2N})_{1J} = |(M_{2,3,4}^{2N})_{1J} - (K_{2,3,4}^{2N})_{1J}|$. As is shown, the lower-left entries of E_2^{2N} , E_3^{2N} , respectively, where we define E_3^{2N} , E_3^{2N} , E_3^{2N} , E_3^{2N} , E_3^{2N} , respectively, where we define E_3^{2N} , E_3^{2N}

as an example. The K-matrix with blocks A and B given by Eq. (35) is denoted as K_3^{2N} , where 2N refers to the size of the K-matrix. As shown in Fig. 6(a2), the braiding phase $2\pi \mathbf{l}_1^{\mathrm{T}}(K_3^{2N})^{-1}\mathbf{l}_{2N}$ between topological excitations residing at distinct z-boundaries oscillates between

0 and 2π as the system size 2N increases, indicating the existence of Toeplitz braiding. This existence can be directly observed from the inverse of K_3^{2N} . The matrix plot of the inverse is shown in Fig. 6(b2), where we consider a system size of 2N=200. K_3^{2N} has only one boundary

zero mode $\mathbf{v}_{3,1}$. We introduce a matrix constructed by the boundary zero mode $\mathbf{v}_{3,1}$:

$$M_3^{2N} = \frac{1}{\lambda_{3,1}} \mathbf{v}_{3,1} \mathbf{v}_{3,1}^{\dagger}. \tag{36}$$

Compared to the inverse of the K_3^{2N} -matrix, M_3^{2N} provides a good approximation to the upper-right and lower-left entries of K_3^{2N} , as depicted in Fig. 6(c2), where we define a matrix $(E_3^{2N})_{IJ} = |(M_3^{2N})_{IJ} - (K_3^{2N})_{IJ}^{-1}|$ to characterize the similarity. As the system size 2N increases, the upper-right and lower-left entries of M_3^{2N} and $(K_3^{2N})^{-1}$ converge towards each other, as shown in Fig. 6(d2), where we focus on the asymptotic behavior of $(E_3^{2N})_{2N,2}$ as an example. This observation suggests that we can extract information about the braiding statistics of excitations residing at distinct z-boundaries by analyzing the zero modes and their close-to-zero eigenvalues.

C. Numerical Computation on Toeplitz Braiding in Type-III Model

To demonstrate the correspondence between boundary zero modes and Toeplitz braiding in Type-III models, we consider the K-matrix of size 2N given by Eq. (2) with

$$A = \begin{pmatrix} 2 & 2 \\ 2 & 0 \end{pmatrix}, \quad B = \begin{pmatrix} 2 & 4 \\ 1 & 2 \end{pmatrix}. \tag{37}$$

as an example. The K-matrix with blocks A and B given by Eq. (39) is denoted as K_4^{2N} , where 2N refers to the size of the K-matrix. As shown in Fig. 6(a3), the braiding phase $2\pi \mathbf{l}_1^{\mathrm{T}}(K_4^{2N})^{-1}\mathbf{l}_{2N}$ between topological excitations residing at distinct z-boundaries oscillates between 0 and 2π as the system size 2N increases, indicating the existence of Toeplitz braiding. This existence can be directly observed from the inverse of K_4^{2N} . The matrix plot of the inverse is shown in Fig. 6(b3), where we consider a system size of 2N=200. K_4^{2N} has only one boundary zero mode $\mathbf{v}_{4,1}$. We introduce a matrix constructed by the boundary zero mode $\mathbf{v}_{4,1}$:

$$M_4^{2N} = \frac{1}{\lambda_{4,1}} \mathbf{v}_{4,1} \mathbf{v}_{4,1}^{\dagger}. \tag{38}$$

Compared to the inverse of the K_4^{2N} -matrix, M_4^{2N} provides a good approximation to the upper-right and lower-left entries of K_4^{2N} , as depicted in Fig. 6(c3), where we define a matrix $(E_4^{2N})_{IJ} = |(M_4^{2N})_{IJ} - (K_4^{2N})_{IJ}^{-1}|$ to characterize the similarity. As the system size 2N increases, the upper-right and lower-left entries of M_4^{2N} and $(K_4^{2N})^{-1}$ converge towards each other, as shown in

Fig. 6(d3), where we focus on the asymptotic behavior of $(E_4^{2N})_{2N,2}$ as an example. This observation suggests that we can extract information about the braiding statistics of excitations residing at distinct z-boundaries by analyzing the zero modes and their close-to-zero eigenvalues.

D. Numerical Computation on Trivial iCS Theory

We also present numerical computation on iCS theories without Toeplitz braiding. We consider the K-matrix of size 2N given by Eq. (2) with

$$A = \begin{pmatrix} 2 & 2 \\ 2 & 0 \end{pmatrix}, \quad B = \begin{pmatrix} 0 & 1 \\ 0 & 0 \end{pmatrix}. \tag{39}$$

as an example, denoted as K_5^{2N} . K_5^{2N} does not possess a boundary zero mode. As shown in Fig. (6)(a4), the braiding phase between topological excitations residing at distinct z-boundaries decreases drastically as the system size 2N increases. Fig. (6)(b4) shows that the upper-right and lower-left elements of $(K_5^{2N})^{-1}$ approach to zero as the system size 2N increases.

V. CONCLUSIONS

In this paper, we proposed a type of topologically ordered non-liquids called "Toeplitz non-liquids" which supports nontrivial Toeplitz braiding. The low energy theory is given by iCS theory with a coefficient matrix called "K-matrix" that is of block-tridiagonal Toeplitz matrix-type. We theoretically analyzed how and when Toeplitz braiding occurs. Especially, the boundary-zeromodes of K-matrices play a critical role. Finally, we numerically studied the three types of K-matrices that support nontrivial Toeplitz braiding. There are several future directions. Following the construction of topologically-ordered non-liquid states in this paper, the construction of higher-dimensional topologically-ordered non-liquid states is directly allowed. For instance, by stacking 3+1D topological orders [51–54], we can obtain a 4+1D topologically-ordered non-liquid state. Similarly, stacking 2+1D topological orders in two independent spatial dimensions can also yield 4+1D topologically-ordered non-liquid states. The study of these theories and the duality between them is left for future research.

ACKNOWLEDGMENTS

This work was supported by National Natural Science Foundation of China (NSFC) Grant No. 12074438 and Guangdong Provincial Key Laboratory of Magnetoelectric Physics and Devices under Grant No. 2022B1212010008.

- [2] Y. Zhou, K. Kanoda, and T.-K. Ng, Quantum spin liquid states, Reviews of Modern Physics 89, 025003 (2017).
- [3] B. Zeng and X.-G. Wen, Gapped quantum liquids and topological order, stochastic local transformations and emergence of unitarity, Physical Review B 91 (2015).
- [4] J. Haah, Local stabilizer codes in three dimensions without string logical operators, Physical Review A 83, 042330 (2011).
- [5] S. Vijay, J. Haah, and L. Fu, Fracton topological order, generalized lattice gauge theory, and duality, Physical Review B 94, 235157 (2016).
- [6] R. M. Nandkishore and M. Hermele, Fractons, Annual Review of Condensed Matter Physics 10, 295 (2019).
- [7] M. Pretko, X. Chen, and Y. You, Fracton phases of matter, International Journal of Modern Physics A 35, 2030003 (2020).
- [8] W. Shirley, K. Slagle, Z. Wang, and X. Chen, Fracton models on general three-dimensional manifolds, Physical Review X 8, 031051 (2018).
- [9] M. Pretko, Subdimensional particle structure of higher rank U(1) spin liquids, Physical Review B 95, 115139 (2017).
- [10] M. Pretko, The fracton gauge principle, Physical Review B 98, 115134 (2018).
- [11] K. Slagle, Foliated quantum field theory of fracton order, Physical Review Letters 126, 101603 (2021).
- [12] M.-Y. Li and P. Ye, Fracton physics of spatially extended excitations, Physical Review B 101, 245134 (2020).
- [13] M.-Y. Li and P. Ye, Fracton physics of spatially extended excitations. ii. polynomial ground state degeneracy of exactly solvable models, Physical Review B 104, 235127 (2021).
- [14] X. Chen, H. T. Lam, and X. Ma, Ground state degeneracy of infinite-component Chern-Simons-Maxwell theories (2023), arXiv:2306.00291 [cond-mat.str-el].
- [15] M.-Y. Li and P. Ye, Hierarchy of entanglement renormalization and long-range entangled states, Physical Review B 107, 115169 (2023).
- [16] N. Seiberg and S.-H. Shao, Exotic symmetries, duality, and fractons in 2+1-dimensional quantum field theory, SciPost Phys. 10, 027 (2021).
- [17] X. G. Wen and A. Zee, Classification of abelian quantum hall states and matrix formulation of topological fluids, Phys. Rev. B 46, 2290 (1992).
- [18] X.-G. Wen and A. Zee, Neutral superfluid modes and "magnetic" monopoles in multilayered quantum hall systems, Physical review letters 69, 1811 (1992).
- [19] X. G. Wen, Mean-field theory of spin-liquid states with finite energy gap and topological orders, Phys. Rev. B 44, 2664 (1991).
- [20] Y.-M. Lu and A. Vishwanath, Theory and classification of interacting integer topological phases in two dimensions: A Chern-Simons approach, Phys. Rev. B 86, 125119 (2012).
- [21] Y.-M. Lu and A. Vishwanath, Classification and properties of symmetry-enriched topological phases: Chern-Simons approach with applications to Z_2 spin liquids, Phys. Rev. B **93**, 155121 (2016).
- [22] P. Ye and X.-G. Wen, Projective construction of twodimensional symmetry-protected topological phases with u(1), so(3), or su(2) symmetries, Phys. Rev. B 87, 195128 (2013).
- [23] Z.-X. Liu, J.-W. Mei, P. Ye, and X.-G. Wen, $u(1) \times u(1)$ symmetry-protected topological order in gutzwiller wave

- functions, Phys. Rev. B 90, 235146 (2014).
- [24] L.-Y. Hung and Y. Wan, K matrix construction of symmetry-enriched phases of matter, Phys. Rev. B 87, 195103 (2013).
- [25] Z.-C. Gu, J. C. Wang, and X.-G. Wen, Multikink topological terms and charge-binding domain-wall condensation induced symmetry-protected topological states: Beyond chern-simons/bf field theories, Phys. Rev. B 93, 115136 (2016).
- [26] M. Cheng and Z.-C. Gu, Topological response theory of abelian symmetry-protected topological phases in two dimensions, Phys. Rev. Lett. 112, 141602 (2014).
- [27] L. Balents and M. P. Fisher, Chiral surface states in the bulk quantum hall effect, Physical review letters 76, 2782 (1996).
- [28] C. L. Kane and M. P. A. Fisher, Impurity scattering and transport of fractional quantum hall edge states, Phys. Rev. B 51, 13449 (1995).
- [29] J. D. Naud, L. P. Pryadko, and S. L. Sondhi, Fractional quantum hall effect in infinite-layer systems, Phys. Rev. Lett. 85, 5408 (2000).
- [30] J. Naud, L. P. Pryadko, and S. Sondhi, Notes on infinite layer quantum hall systems, Nuclear Physics B 594, 713 (2001).
- [31] D. P. Druist, P. J. Turley, K. D. Maranowski, E. G. Gwinn, and A. C. Gossard, Observation of chiral surface states in the integer quantum hall effect, Phys. Rev. Lett. 80, 365 (1998).
- [32] X. Qiu, R. Joynt, and A. MacDonald, Phases of the multiple quantum well in a strong magnetic field: Possibility of irrational charge, Physical Review B 40, 11943 (1989).
- [33] X. Ma, W. Shirley, M. Cheng, M. Levin, J. McGreevy, and X. Chen, Fractonic order in infinite-component Chern-Simons gauge theories, Physical Review B 105 (2022).
- [34] X. Chen, H. T. Lam, and X. Ma, Gapless infinitecomponent Chern-Simons-Maxwell theories (2022), arXiv:2211.10458 [cond-mat.str-el].
- [35] J. Sullivan, A. Dua, and M. Cheng, Weak symmetry breaking and topological order in a 3d compressible quantum liquid (2021), arXiv:2109.13267 [cond-mat.str-el].
- [36] J. Sullivan, T. Iadecola, and D. J. Williamson, Planar p-string condensation: Chiral fracton phases from fractional quantum hall layers and beyond, Phys. Rev. B 103, 205301 (2021).
- [37] C. H. Lee and P. Ye, Free-fermion entanglement spectrum through wannier interpolation, Physical Review B 91, 085119 (2015).
- [38] G. Meurant, A review on the inverse of symmetric tridiagonal and block tridiagonal matrices, SIAM Journal on Matrix Analysis and Applications 13, 707 (1992).
- [39] J. I. I. Hirschman, Matrix-valued Toeplitz operators, Duke Mathematical Journal 34, 403 (1967).
- [40] S.-E. Ekström and S. Serra-Capizzano, Eigenvalues and eigenvectors of banded toeplitz matrices and the related symbols, Numerical Linear Algebra with Applications 25, e2137 (2018).
- [41] M. Wax and T. Kailath, Efficient inversion of toeplitzblock toeplitz matrix, IEEE transactions on acoustics, speech, and signal processing 31, 1218 (1983).
- 42] J. Gutiérrez-Gutiérrez, P. M. Crespo, et al., Block toeplitz matrices: Asymptotic results and applications, Foundations and Trends® in Communications and Information Theory 8, 179 (2012).

- [43] G. Heinig and K. Rost, Algebraic methods for Toeplitzlike matrices and operators, Vol. 13 (Birkhäuser Basel, 1984).
- [44] W. P. Su, J. R. Schrieffer, and A. J. Heeger, Soliton excitations in polyacetylene, Phys. Rev. B 22, 2099 (1980).
- [45] X.-L. Qi and S.-C. Zhang, Topological insulators and superconductors, Rev. Mod. Phys. 83, 1057 (2011).
- [46] H.-M. Guo, A brief review on one-dimensional topological insulators and superconductors, Science China Physics, Mechanics & Astronomy 59, 1 (2016).
- [47] A. Y. Kitaev, Unpaired Majorana fermions in quantum wires, Physics-Uspekhi 44, 131–136 (2001).
- [48] S.-Q. Shen, Topological insulators, Vol. 174 (Springer, 2012).
- [49] J. K. Asbóth, L. Oroszlány, and A. Pályi, A short course on topological insulators, Vol. 919 (Springer, 2016) p. 166.
- [50] R. Movassagh, G. Strang, Y. Tsuji, and R. Hoffmann, The green's function for the Hückel (tight binding) model, Journal of Mathematical Physics 58 (2017).
- [51] Z.-F. Zhang and P. Ye, Compatible braidings with hopf links, multiloop, and borromean rings in (3 + 1)-dimensional spacetime, Phys. Rev. Res. 3, 023132 (2021).
- [52] Z.-F. Zhang, Q.-R. Wang, and P. Ye, Continuum field theory of three-dimensional topological orders with emergent fermions and braiding statistics, Physical Review Research 5, 043111 (2023).
- [53] Z.-F. Zhang, Q.-R. Wang, and P. Ye, Non-abelian fusion, shrinking, and quantum dimensions of abelian gauge fluxes, Physical Review B 107, 165117 (2023).
- [54] Y. Huang, Z.-F. Zhang, and P. Ye, Diagrammatic Representations of Higher-Dimensional Topological Orders, arXiv e-prints, arXiv:2405.19077 (2024), arXiv:2405.19077 [hep-th].

Appendix A: Detailed Derivation on Sorting Zero Modes of K-matrices

1.
$$\det B = 0$$

If $l_4 \neq 0$, for ϕ^1 , the bulk recurrence relation Eq. (20) is solved by

$$\phi^{1,A} = l_4(1+\beta_1^2)\phi_1, \quad \phi^{1,B} = -(l_3+m\beta_1+l_2\beta_1^2)\phi_1.$$

 $\phi_1 \in \mathbb{R}$ is a normalization constant. ϕ^1 is required to satisfy boundary condition Eq. (17a), which gives

$$\begin{pmatrix}
\beta_1 \left(\beta_1 \left(\beta_1^2 + 1\right) l_1 l_4 - m(\beta_1 (\beta_1 l_2 + m) + l_3) - \beta_1 l_3 (\beta_1 (\beta_1 l_2 + m) + l_3) + \left(\beta_1^2 + 1\right) l_4 n\right) \\
\beta_1 l_4 (\beta_1 (l_2 - l_3) + m)
\end{pmatrix} \phi_1 = 0 \tag{A1}$$

We consider the constraints on the entries of K implied by $\beta_1 l_4(\beta_1(l_2 - l_3) + m) = 0$. If $l_4 \neq 0$, the equation $\beta_1 l_4(\beta_1(l_2 - l_3) + m) = 0$ implies $\beta_1(l_2 - l_3) + m = 0$. This equation can be further divided into two subcases:

Case 1: $l_2 = l_3$ and m = 0

Case 2: $\beta_1 = \frac{m}{l_3 - l_2}$

In Case 1, we have $|\beta_1| = 1$, which does not correspond to a boundary state and should be discarded. Hence we shall continue with Case 2. Since $l_4 \neq 0$, we can safely set $l_1 = l_2 l_3 / l_4$. Eq. (A1) renders

$$\frac{m\left((l_2 - l_3)^2 + m^2\right)}{(l_2 - l_3)^3}(2l_3m - l_4n) = 0$$

Therefore, if $2l_3m - l_4n = 0$, Eq. (19) represents a boundary state that satisfies the boundary condition Eq. (17a). Taking into account the aforementioned conditions, if

$$\begin{cases} m \neq 0 \\ l_4 \neq 0 \\ l_1 l_4 = l_2 l_3 \\ 2 l_3 m = l_4 n \\ |m| < |l_3 - l_2| \end{cases},$$

then there exists one boundary zero mode ϕ^1 given by Eq. (19), where

$$\phi^{1,A} = \frac{l_4}{\sqrt{l_3^2 + l_4^2}} \sqrt{\frac{1 - \beta_1^2}{1 - \beta_1^{2N}}}, \quad \phi^{1,B} = -\frac{l_3}{\sqrt{l_3^2 + l_4^2}} \sqrt{\frac{1 - \beta_1^2}{1 - \beta_1^{2N}}}$$

The above discussion has ignored the case where $l_4 = 0$. If $l_4 = 0$, det B = 0 enforces $l_2 l_3 = 0$. The discussion is similar. If $l_2 = 0$, $l_3 \neq 0$, i.e.

$$A = \begin{pmatrix} n & m \\ m & 0 \end{pmatrix}, \quad B = \begin{pmatrix} l_1 & 0 \\ l_3 & 0 \end{pmatrix}$$

For ϕ^1 , Eq. (20) is solved by

$$\phi^{1,A} = 0, \quad \phi^{1,B} = \phi_1, \tag{A2}$$

where $\phi_1 \in \mathbb{R}$ is the normalization constant. ϕ^1 is required to satisfy the boundary condition Eq. (17a), which gives

$$\begin{pmatrix} \beta_1^2 l_1 + \beta_1 n & \beta_1^2 l_3 + \beta_1 m \\ \beta_1 m & 0 \end{pmatrix} \begin{pmatrix} \phi^{1,A} \\ \phi^{1,B} \end{pmatrix} = 0$$
 (A3)

If ϕ^1 is solved by Eq. (A2), $\beta_1 = -\frac{m}{l_3}$, Eq. (A3) naturally holds. Therefore, if

$$\begin{cases} m \neq 0 \\ l_3 \neq 0 \\ l_4 = l_2 = 0 \\ |m| < |l_3| \end{cases}$$

there exists a boundary zero mode ϕ^1 with

$$\phi^{1,A} = 0, \quad \phi^{1,B} = \sqrt{\frac{1 - \beta_1^{2N}}{1 - \beta_1^2}} \tag{A4}$$

satisfying boundary condition Eq. (17a). If $l_3 = 0$, $l_2 \neq 0$ i.e.

$$A = \begin{pmatrix} n & m \\ m & 0 \end{pmatrix}, \quad B = \begin{pmatrix} l_1 & l_2 \\ 0 & 0 \end{pmatrix},$$

the bulk recurrence relation Eq. (20) is solved by

$$\begin{cases} \phi^{1,A} = 0 \\ \phi^{1,B} = \phi_1 \\ \beta_1 = -\frac{l_2}{m} \end{cases} \text{ or } \begin{cases} \phi^{1,A} = -l_2(l_2^2 - m^2)\phi_1 \\ \phi^{1,B} = (l_1(l_2^2 + m^2) - l_2mn)\phi_1 \\ \beta_1 = -\frac{m}{l_2} \end{cases}$$

However, none of these solutions satisfy the boundary condition Eq. (17a). Likewise, for ϕ^2 , the bulk recurrence relation Eq. (20) is solved by

$$\phi^{2,A} = l_4(1+\beta_2^2)\phi_2, \quad \phi^{2,B} = -(l_3 + m\beta_2 + l_2\beta_2^2)\phi_2,$$

where $\phi_2 \in \mathbb{R}$ is a normalization constant. It is required to satisfy the boundary condition Eq. (17b), rendering

$$\left(-\left(-\left(\beta_2^2 + 1 \right) l_4(l_1 + n\beta_2) + \beta_2^2 l_2^2 + l_2 \left(l_3 + \beta_2 m + \beta_2^3 m \right) + \beta_2^2 m(l_3 + \beta_2 m) \right) \phi_2 = 0$$
(A5)

Eq. (A5) implies $l_4((l_3-l_2)+m\beta_2)=0$, which gives $\beta_2=\frac{l_2-l_3}{m}$. If $l_4\neq 0$, we can safely set $l_1=l_2l_3/l_4$. Substituting $\beta_2=\frac{l_2-l_3}{m}$ into Eq. (A5), it gives

$$\frac{\left((l_2 - l_3)^2 + m^2\right)(2l_2m - l_4n)}{(l_2 - l_3)^2} = 0$$

Therefore, if $2l_2m - l_4n = 0$, (19) represents a boundary state that satisfies the boundary condition (17b). Taking the aforementioned conditions into account, if

$$\begin{cases} m \neq 0 \\ l_4 \neq 0 \\ l_1 l_4 = l_2 l_3 \\ 2 l_2 m = l_4 n \\ |m| < |l_3 - l_2| \end{cases},$$

then there exists one boundary state (19), where $\beta_2 = \frac{l_2 - l_3}{m}$

$$\phi^{2,A} = \frac{l_4}{\sqrt{l_2^2 + l_4^2}} \sqrt{\frac{1 - \beta_2^2}{1 - \beta_2^{2N}}}, \quad \phi^{2,B} = -\frac{l_2}{\sqrt{l_2^2 + l_4^2}} \sqrt{\frac{1 - \beta_2^2}{1 - \beta_2^{2N}}}$$

The above discussion has ignored the case where $l_4=0$. If $l_4=0$, $\det B=0$ enforces $l_2l_3=0$. The discussion is similar. If $l_3=0$, $l_2\neq 0$ i.e.

$$A = \begin{pmatrix} n & m \\ m & 0 \end{pmatrix}, \quad B = \begin{pmatrix} l_1 & l_2 \\ 0 & 0 \end{pmatrix}$$

For ϕ^2 , Eq. (20) is solved by

$$\phi^{2,A} = 0, \quad \phi^{2,B} = \phi_2, \quad \beta_2 = -\frac{l_2}{m}$$
 (A6)

where $\phi_2 \in \mathbb{R}$ is a normalization constant. ϕ^2 is required to satisfy the boundary condition Eq. (17b), which gives

$$\begin{pmatrix} l_1 + \beta_2 n & l_2 + \beta_2 m \\ \beta_2 m & 0 \end{pmatrix} \begin{pmatrix} \phi^{2,A} \\ \phi^{2,B} \end{pmatrix} = 0 \tag{A7}$$

If ϕ^2 is solved by (A6), Eq. (A7) naturally holds. Therefore, if

$$\begin{cases} m \neq 0 \\ l_2 \neq = 0 \\ l_4 = l_3 = 0 \\ |m| < |l_2| \end{cases},$$

there exists a boundary zero mode ϕ^2 with

$$\phi^{2,A} = 0, \quad \phi^{2,B} = \sqrt{\frac{1 - \beta_2^{2N}}{1 - \beta_2^2}}$$
 (A8)

satisfying the boundary condition Eq. (17b). If $l_2 = 0$, $l_3 \neq 0$ i.e.

$$A = \begin{pmatrix} n & m \\ m & 0 \end{pmatrix}, \quad B = \begin{pmatrix} l_1 & 0 \\ l_3 & 0 \end{pmatrix}$$

the bulk recurrence relation Eq. (20) is solved by

$$\begin{cases} \phi^{2,A} = 0 \\ \phi^{2,B} = \phi_2 \\ \beta_2 = -\frac{l_3}{m} \end{cases} \text{ or } \begin{cases} \phi^{2,A} = -(m\beta_2 + l_3\beta_2^2)\phi_2 \\ \phi^{2,B} = (l_1 + n\beta_2 + l_1\beta_2^2)\phi_2 \\ \beta_2 = -\frac{l_3}{m} \end{cases}$$

However, none of these solutions satisfy the boundary condition Eq. (17b). In summary, if

$$\begin{cases}
 m \neq 0 \\
 n \neq 0 \\
 l_1 l_4 = l_2 l_3 \\
 2 l_2 m = l_4 n \text{ or } 2 l_3 m = l_4 n \\
 |m| < |l_3 - l_2|
\end{cases} , \tag{A9}$$

there exists one boundary zero mode. If

$$\begin{cases}
 m \neq 0 \\
 n = 0 \\
 l_1 = l_3 = l_4 = 0 \text{ or } l_1 = l_2 = l_4 = 0 \\
 |m| < |l_3| \text{ or } |m| < |l_2|
\end{cases}$$
(A10)

there exist two boundary zero modes.

2.
$$\det B \neq 0$$

If det $B=l_1l_4-l_2l_3\neq 0$, Eq. (22) is a fourth-degree equation. In accordance to the main text, denote $l_1l_4-l_2l_3$ as $a,-(m(l_2+l_3)-nl_4)$ as $b,-(l_2^2+l_3^2-2l_1l_4+m^2)$ as c. If det $B=l_1l_4-l_2l_3\neq 0$, the solution of β is

$$\beta_1 = \frac{-a\sqrt{\frac{2b\left(\sqrt{8a^2 - 4ac + b^2} + b\right) - 4ac}{a^2} - 8} - \sqrt{8a^2 - 4ac + b^2} - b}}{\frac{4a}{}},$$

$$\beta_2 = \frac{a\sqrt{\frac{2b\left(\sqrt{8a^2 - 4ac + b^2} + b\right) - 4ac}{a^2} - 8} - \sqrt{8a^2 - 4ac + b^2} - b}}{\frac{4a}{}},$$

$$\beta_3 = \frac{-a\sqrt{\frac{2b\left(b - \sqrt{8a^2 - 4ac + b^2}\right) - 4ac}{a^2} - 8} + \sqrt{8a^2 - 4ac + b^2} - b}}{\frac{4a}{}},$$

$$\beta_4 = \frac{a\sqrt{\frac{2b\left(b - \sqrt{8a^2 - 4ac + b^2}\right) - 4ac}{a^2} - 8} + \sqrt{8a^2 - 4ac + b^2} - b}}{\frac{4a}{}},$$

The solution gives

$$\beta_1 \beta_2 = 1, \quad \beta_3 \beta_4 = 1.$$
 (A11)

If $l_4 \neq 0$, there is a significant challenge in seeking a comprehensive analytical solution. To simplify discussion, we focus on the special case where $l_4 = 0$. Set $l_4 = 0$. Eq. (22) gives

$$(l_2 + m\beta + l_3\beta^2)(l_3 + m\beta + l_2\beta^2) = 0$$
(A12)

Since det B=0 has been discussed, we assume that det $B=l_2l_3\neq 0$. Solutions to (A12) are

$$\beta_1 = \frac{-m - \sqrt{m^2 - 4l_2 l_3}}{2l_3}$$

$$\beta_3 = \frac{-m + \sqrt{m^2 - 4l_2 l_3}}{2l_3}$$

$$\beta_2 = \frac{-m + \sqrt{m^2 - 4l_2 l_3}}{2l_2}$$

$$\beta_4 = \frac{-m - \sqrt{m^2 - 4l_2 l_3}}{2l_2}$$

 β_1 and β_3 are solutions to $l_2 + m\beta + l_3\beta^2 = 0$. β_4 and β_2 are solutions to $l_3 + m\beta + l_2\beta^2 = 0$. $\beta_1\beta_2 = 1$, $\beta_3\beta_4 = 1$. It can be readily verified that if $|\beta_1| = |\beta_2| = 1$, then $|\beta_3| = |\beta_4| = 1$. Similarly, if $|\beta_3| = |\beta_4| = 1$, then $|\beta_1| = |\beta_2| = 1$. Therefore, we only need to consider 4 cases:

Case I. $|\beta_1| > 1$, $|\beta_2| < 1$, $|\beta_3| > 1$, $|\beta_4| < 1$.

Case II. $|\beta_1| > 1$, $|\beta_2| < 1$, $|\beta_3| < 1$, $|\beta_4| > 1$.

Case III. $|\beta_1| < 1$, $|\beta_2| > 1$, $|\beta_3| > 1$, $|\beta_4| < 1$.

Case IV. $|\beta_1| < 1$, $|\beta_2| > 1$, $|\beta_3| < 1$, $|\beta_4| > 1$.

Case I. Denote the eigenvector corresponding to β_2 and β_4 as ϕ^2 and ϕ^4 , respectively.

$$\phi^{2} = (\beta_{2}\phi^{2,A} \ \beta_{2}\phi^{2,B} \ \beta_{2}^{2}\phi^{2,A} \ \beta_{2}^{2}\phi^{2,B} \ \cdots \ \beta_{2}^{N}\phi^{2,A} \ \beta_{2}^{N}\phi^{2,B})^{\mathrm{T}}$$

$$\phi^{4} = (\beta_{4}\phi^{4,A} \ \beta_{4}\phi^{4,B} \ \beta_{4}^{2}\phi^{4,A} \ \beta_{4}^{2}\phi^{4,B} \ \cdots \ \beta_{4}^{N}\phi^{4,A} \ \beta_{4}^{N}\phi^{4,B})^{\mathrm{T}}$$

The bulk recurrence relation Eq. (20) gives

$$\begin{pmatrix} l_1 + n\beta_j + l_1\beta_j^2 & l_2 + m\beta_j + l_3\beta_j^2 \\ 0 & 0 \end{pmatrix} \begin{pmatrix} \phi^{j,A} \\ \phi^{j,B} \end{pmatrix} = 0, \quad j = 2, 4$$

Set

$$\phi^{j,A} = (l_2 + m\beta_j + l_3\beta_j^2)\phi_j$$
$$\phi^{j,B} = -(l_1 + n\beta_j + l_1\beta_j^2)\phi_j$$

where $\phi_j \in \mathbb{R}$ is normalization constant. A potential solution $\psi^{2,4}$

$$\boldsymbol{\psi}^{2,4} = \left(\psi_1^{2,4,A} \ \psi_1^{2,4,B} \ \psi_2^{2,4,A} \ \psi_2^{2,4,B} \ \cdots \ \psi_N^{2,4,A} \ \psi_N^{2,4,B}\right)^{\mathrm{T}}$$

is a linear combination of ϕ^2 and ϕ^4 .

$$\begin{pmatrix} \psi_{l}^{2,4,A} \\ \psi_{l}^{2,4,B} \end{pmatrix} = \beta_{2}^{l} \begin{pmatrix} l_{2} + m\beta_{2} + l_{3}\beta_{2}^{2} \\ -(l_{1} + n\beta_{2} + l_{1}\beta_{2}^{2}) \end{pmatrix} \phi_{2} + \beta_{4}^{l} \begin{pmatrix} l_{2} + m\beta_{4} + l_{3}\beta_{4}^{2} \\ -(l_{1} + n\beta_{4} + l_{1}\beta_{4}^{2}) \end{pmatrix} \phi_{4}$$

 $\phi_2, \phi_4 \in \mathbb{R}$. We discuss the condition $\beta_2 \neq \beta_4$ at first. $\beta_2 \neq \beta_4$ implies $m^2 \neq 4l_1l_2$. Since $|\beta_2| < 1$, $|\beta_4| < 1$, $|\psi^{2,4}|$ is required to satisfy the boundary condition Eq. (17a), which renders

$$\left(\begin{array}{ccc} r_1 & r_2 \\ \beta_2^2 l_2 \left(l_2 + \beta_2^2 l_3 + \beta_2 m \right) + \beta_2 m \left(l_2 + \beta_2^2 l_3 + \beta_2 m \right) & \beta_4^2 l_2 \left(l_2 + \beta_4^2 l_3 + \beta_4 m \right) + \beta_4 m \left(l_2 + \beta_4^2 l_3 + \beta_4 m \right) \end{array} \right) \begin{pmatrix} \phi_2 \\ \phi_4 \end{pmatrix} = 0,$$

where

$$r_{1} = \beta_{2}^{2} l_{1} \left(l_{2} + \beta_{2}^{2} l_{3} + \beta_{2} m \right) + \beta_{2}^{2} l_{3} \left(\beta_{2}^{2} (-l_{1}) - l_{1} - \beta_{2} n \right) + \beta_{2} m \left(\beta_{2}^{2} (-l_{1}) - l_{1} - \beta_{2} n \right) + \beta_{2} n \left(l_{2} + \beta_{2}^{2} l_{3} + \beta_{2} m \right),$$

$$r_{2} = \beta_{4}^{2} l_{1} \left(l_{2} + \beta_{4}^{2} l_{3} + \beta_{4} m \right) + \beta_{4}^{2} l_{3} \left(\beta_{4}^{2} (-l_{1}) - l_{1} - \beta_{4} n \right) + \beta_{4} m \left(\beta_{4}^{2} (-l_{1}) - l_{1} - \beta_{4} n \right) + \beta_{4} n \left(l_{2} + \beta_{4}^{2} l_{3} + \beta_{4} m \right).$$

Nontrivial solution to ϕ_2 , ϕ_4 renders

$$(l_2 - l_3)(n(l_2 + l_3) - 2l_1m) = 0$$

 $l_2 = l_3$ renders either $|\beta_2| |\beta_4| = 1$ or $|\beta_2| = |\beta_4| = 1$, which is out of consideration. Therefore, if $n(l_2 + l_3) = 2l_1 m$, there exists a boundary state satisfying boundary condition Eq. (17a).

The above discussion has ignored $m^2 = 4l_2l_3$. Detailed calculations reveal that in this condition, $|\beta_2| = |\beta_4| = 1$, which contradicts the assumption that $|\beta_2| < 1$, $|\beta_4| < 1$.

The next step is the discussion on eigenvectors corresponding to β_1 and β_4 . Denote the eigenvectors corresponding to β_1 and β_3 as ϕ^1 and ϕ^3 , respectively.

$$\phi^{1} = (\beta_{1}\phi^{1,A} \ \beta_{1}\phi^{1,B} \ \beta_{1}^{2}\phi^{1,A} \ \beta_{1}^{2}\phi^{1,B} \ \cdots \ \beta_{1}^{N}\phi^{1,A} \ \beta_{1}^{N}\phi^{1,B})^{T}$$

$$\phi^{3} = (\beta_{3}\phi^{3,A} \ \beta_{3}\phi^{3,B} \ \beta_{3}^{2}\phi^{3,A} \ \beta_{3}^{2}\phi^{3,B} \ \cdots \ \beta_{3}^{N}\phi^{3,A} \ \beta_{3}^{N}\phi^{3,B})^{T}$$

The bulk recurrence relation Eq. (20) gives

$$\begin{pmatrix} l_1 + n\beta_j + l_1\beta_j^2 & 0 \\ l_3 + m\beta_j + l_2\beta_j^2 & 0 \end{pmatrix} \begin{pmatrix} \phi^{j,A} \\ \phi^{j,B} \end{pmatrix} = 0, \quad j = 1, 3$$

Set

$$\phi^{j,A} = 0, \quad \phi^{j,B} = \phi_j$$

A potential solution $\psi^{1,3}$ is a linear combination of ϕ^1 and ϕ^3 .

$$\boldsymbol{\psi}^{1,3} = \begin{pmatrix} \psi_1^{1,3,A} & \psi_1^{1,3,B} & \psi_2^{1,3,A} & \psi_2^{1,3,B} & \cdots & \psi_N^{1,3,A} & \psi_N^{1,3,B} \end{pmatrix}^{\mathrm{T}} \begin{pmatrix} \psi_l^{1,3,A} \\ \psi_l^{1,3,B} \end{pmatrix} = \beta_1^l \begin{pmatrix} 0 \\ 1 \end{pmatrix} \phi_1 + \beta_3^l \begin{pmatrix} 0 \\ 1 \end{pmatrix} \phi_3$$

If $\beta_1 \neq \beta_3 \Leftrightarrow m^2 \neq 4l_1l_2$, the boundary condition (17b) renders

$$\begin{pmatrix} \beta_1^{N-1}(l_2 + \beta_1 m) & \beta_3^{N-1}(l_2 + \beta_3 m) \\ 0 & 0 \end{pmatrix} \begin{pmatrix} \phi_1 \\ \phi_3 \end{pmatrix} = 0$$
 (A13)

(A13) always has nontrivial solution. Therefore, there always exist boundary states satisfying the boundary condition (17b). If $m^2 = 4l_2l_3$, $\beta_1 = \beta_3 = \frac{-m}{2l_3}$, the condition for nontrivial solution is

$$B\begin{pmatrix} \psi_{N-1}^{1,3,A} \\ \psi_{N-1}^{1,3,B} \end{pmatrix} + A\begin{pmatrix} \psi_{N}^{1,3,A} \\ \psi_{N}^{1,3,B} \end{pmatrix} = 0$$

Detailed calculation shows that there is no solution.

Case II. Denote the eigenvector corresponding to β_2 and β_3 as ϕ^2 and ϕ^3 , respectively.

$$\phi^{2} = \begin{pmatrix} \beta_{2}\phi^{2,A} & \beta_{2}\phi^{2,B} & \beta_{2}^{2}\phi^{2,A} & \beta_{2}^{2}\phi^{2,B} & \cdots & \beta_{2}^{N}\phi^{2,A} & \beta_{2}^{N}\phi^{2,B} \end{pmatrix}^{T}$$
$$\phi^{3} = \begin{pmatrix} \beta_{3}\phi^{3,A} & \beta_{3}\phi^{3,B} & \beta_{3}^{2}\phi^{3,A} & \beta_{3}^{2}\phi^{3,B} & \cdots & \beta_{3}^{N}\phi^{3,A} & \beta_{3}^{N}\phi^{3,B} \end{pmatrix}^{T}$$

The bulk recurrence relation Eq. (20) gives

$$\begin{pmatrix} l_1 + n\beta_2 + l_1\beta_2^2 & l_2 + m\beta_2 + l_3\beta_2^2 \\ 0 & 0 \end{pmatrix} \begin{pmatrix} \phi^{2,A} \\ \phi^{2,B} \end{pmatrix} = 0$$
$$\begin{pmatrix} l_1 + n\beta_3 + l_1\beta_3^2 & 0 \\ l_3 + m\beta_3 + l_2\beta_3^2 & 0 \end{pmatrix} \begin{pmatrix} \phi^{3,A} \\ \phi^{3,B} \end{pmatrix} = 0$$

Set

$$\begin{cases} \phi^{2,A} = (l_2 + m\beta_2 + l_3\beta_2^2)\phi_2 \\ \phi^{2,B} = -(l_1 + n\beta_2 + l_1\beta_2^2)\phi_2 \\ \phi^{3,A} = 0 \\ \phi^{3,B} = \phi_3 \end{cases}$$

A potential solution is a linear combination of ϕ^2 and ϕ^3 .

$$\psi^{2,3} = \left(\psi_1^{2,3,A} \ \psi_1^{2,3,B} \ \psi_2^{2,3,A} \ \psi_2^{2,3,B} \ \cdots \ \psi_N^{2,3,A} \ \psi_N^{2,3,B}\right)^{\mathrm{T}}$$
$$\begin{pmatrix} \psi_l^{2,3,A} \\ \psi_l^{2,3,B} \end{pmatrix} = \beta_2^l \begin{pmatrix} l_2 + m\beta_2 + l_3\beta_2^2 \\ -(l_1 + n\beta_2 + l_1\beta_2^2) \end{pmatrix} \phi_2 + \beta_3^l \begin{pmatrix} 0 \\ 1 \end{pmatrix} \phi_3$$

 $\phi_2, \phi_3 \in \mathbb{R}$. If $\beta_2 \neq \beta_3 \Leftrightarrow l_2 \neq l_3$, the boundary condition (17a) renders

$$\begin{pmatrix} \beta_2 l_2 n - \beta_2 l_1 (\beta_2 (l_3 - l_2) + m) & \beta_3 (\beta_3 l_3 + m) \\ \beta_2 (\beta_2 l_2 + m) (l_2 + \beta_2 (\beta_2 l_3 + m)) & 0 \end{pmatrix} \begin{pmatrix} \phi_2 \\ \phi_3 \end{pmatrix} = 0$$

Nontrivial solution to the above equation requires

$$\left(m\left(\sqrt{m^2 - 4l_2l_3} - m\right) + 2l_2(l_2 + l_3)\right) = 0$$

If $\beta_2 = \beta_3$ the condition for nontrivial solution is

$$A \begin{pmatrix} \psi_1^{2,3,A} \\ \psi_1^{2,3,B} \end{pmatrix} + B^{\mathrm{T}} \begin{pmatrix} \psi_2^{2,3,A} \\ \psi_2^{2,3,B} \end{pmatrix} = 0 \tag{A14}$$

Detailed calcuation shows that there is no solution to (A14).

Denote the eigenvector corresponding to β_1 and β_4 as ψ^1 and ψ^4 , respectively.

$$\phi^{1} = (\beta_{1}\phi^{1,A} \ \beta_{1}\phi^{1,B} \ \beta_{1}^{2}\phi^{1,A} \ \beta_{1}^{2}\phi^{1,B} \ \cdots \ \beta_{1}^{N}\phi^{1,A} \ \beta_{1}^{N}\phi^{1,B})^{T}$$

$$\phi^{4} = (\beta_{4}\phi^{4,A} \ \beta_{4}\phi^{4,B} \ \beta_{4}^{2}\phi^{4,A} \ \beta_{4}^{2}\phi^{4,B} \ \cdots \ \beta_{4}^{N}\phi^{4,A} \ \beta_{4}^{N}\phi^{4,B})^{T}$$

The bulk recurrence relation Eq. (20) gives

$$\begin{pmatrix} l_1 + n\beta_1 + l_1\beta_1^2 & 0 \\ l_3 + m\beta_1 + l_2\beta_1^2 & 0 \end{pmatrix} \begin{pmatrix} \phi^{1,A} \\ \phi^{1,B} \end{pmatrix} = 0$$
$$\begin{pmatrix} l_1 + n\beta_4 + l_1\beta_4^2 & l_2 + m\beta_4 + l_3\beta_4^2 \\ 0 & 0 \end{pmatrix} \begin{pmatrix} \phi^{4,A} \\ \phi^{4,B} \end{pmatrix} = 0$$

Set

$$\begin{cases} \phi^{1,A} = 0 \\ \phi^{1,B} = \phi_1 \end{cases}$$
$$\begin{cases} \phi^{4,A} = (l_2 + m\beta_4 + l_3\beta_4^2)\phi_4 \\ \phi^{4,B} = -(l_1 + n\beta_4 + l_1\beta_4^2)\phi_4 \end{cases}$$

 $\phi_1, \phi_4 \in \mathbb{R}$. A potential solution $\psi^{1,4}$ is a linear combination of ψ^1 and ψ^4

$$\boldsymbol{\psi}^{1,4} = \begin{pmatrix} \psi_1^{1,4,A} & \psi_1^{1,4,B} & \psi_2^{1,4,A} & \psi_2^{1,4,B} & \cdots & \psi_N^{1,4,A} & \psi_N^{1,4,B} \end{pmatrix}^{\mathrm{T}} \\ \begin{pmatrix} \psi_l^{1,4,A} \\ \psi_l^{1,4,B} \end{pmatrix} = \beta_1^l \begin{pmatrix} 0 \\ 1 \end{pmatrix} \phi_1 + \beta_4^l \begin{pmatrix} l_2 + m\beta_4 + l_3\beta_4^2 \\ -(l_1 + n\beta_4 + l_1\beta_4^2) \end{pmatrix} \phi_4$$

If $\beta_2 \neq \beta_3 \Leftrightarrow l_2 \neq l_3$, the boundary condition (17b) renders

$$\begin{pmatrix} \beta_1^{N-1}(l_2+\beta_1 m) & \beta_4^{N+1}(\beta_4 l_3 n - l_1(l_2 - l_3 + \beta_4 m)) \\ 0 & \beta_4^{N-1}(l_3 + \beta_4 m)(l_2 + \beta_4(\beta_4 l_3 + m)) \end{pmatrix} \begin{pmatrix} \phi_1 \\ \phi_4 \end{pmatrix} = 0$$

Nontrivial solution to the boundary condition (17b) requires

$$(2l_2(l_2+l_3) - m(\sqrt{m^2 - 4l_2l_3} + m)) \left(m\left(\sqrt{m^2 - 4l_2l_3} + m\right) - 2l_2l_3 \right)^2 = 0$$
(A15)

(A15) does not have a solution. If $\beta_1 = \beta_4 \Leftrightarrow l_2 = l_3$, the condition for nontrivial solution is

$$B\begin{pmatrix} \psi_{N-1}^{1,4,A} \\ \psi_{N-1}^{1,4,B} \end{pmatrix} + A\begin{pmatrix} \psi_{N}^{1,4,A} \\ \psi_{N}^{1,4,B} \end{pmatrix} = 0$$

There is no solution in this condition.

Case III. $|\beta_1| < 1$, $|\beta_2| > 1$, $|\beta_3| > 1$, $|\beta_4| < 1$.

Denote the eigenvector corresponding to β_1 and β_4 as ϕ^1 and ϕ^4 , respectively.

$$\phi^{1} = (\beta_{1}\phi^{1,A} \ \beta_{1}\phi^{1,B} \ \beta_{1}^{2}\phi^{1,A} \ \beta_{1}^{2}\phi^{1,B} \ \cdots \ \beta_{1}^{N}\phi^{1,A} \ \beta_{1}^{N}\phi^{1,B})^{T}$$

$$\phi^{4} = (\beta_{4}\phi^{4,A} \ \beta_{4}\phi^{4,B} \ \beta_{4}^{2}\phi^{4,A} \ \beta_{4}^{2}\phi^{4,B} \ \cdots \ \beta_{4}^{N}\phi^{4,A} \ \beta_{4}^{N}\phi^{4,B})^{T}$$

The bulk recurrence relation Eq. (20) gives

$$\begin{pmatrix} l_1 + n\beta_1 + l_1\beta_1^2 & 0 \\ l_3 + m\beta_1 + l_2\beta_1^2 & 0 \end{pmatrix} \begin{pmatrix} \phi^{1,A} \\ \phi^{1,B} \end{pmatrix} = 0$$

$$\begin{pmatrix} l_1 + n\beta_4 + l_1\beta_4^2 & l_2 + m\beta_4 + l_3\beta_4^2 \\ 0 & 0 \end{pmatrix} \begin{pmatrix} \phi^{4,A} \\ \phi^{4,B} \end{pmatrix} = 0$$

Set

$$\begin{cases} \phi^{1,A} = 0 \\ \phi^{1,B} = \phi_1 \end{cases}$$
$$\begin{cases} \phi^{4,A} = (l_2 + m\beta_4 + l_3\beta_4^2)\phi_4 \\ \phi^{4,B} = -(l_1 + n\beta_4 + l_1\beta_4^2)\phi_4 \end{cases}$$

 $\phi_1, \phi_4 \in \mathbb{R}$. A potential solution is a linear combination of ψ^1 and ψ^4 .

$$\psi^{1,4} = \begin{pmatrix} \psi_1^{1,4,A} & \psi_1^{1,4,B} & \psi_2^{1,4,A} & \psi_2^{1,4,B} & \cdots & \psi_N^{1,4,A} & \psi_N^{1,4,B} \end{pmatrix}^{\mathrm{T}} \begin{pmatrix} \psi_l^{1,4,A} \\ \psi_l^{1,4,B} \end{pmatrix} = \beta_1^l \begin{pmatrix} 0 \\ 1 \end{pmatrix} \phi_1 + \beta_4^l \begin{pmatrix} l_2 + m\beta_4 + l_3\beta_4^2 \\ -(l_1 + n\beta_4 + l_1\beta_4^2) \end{pmatrix} \phi_4$$

If $\beta_1 \neq \beta_4 \Leftrightarrow l_2 \neq l_3$, the boundary condition (17a) renders

$$\begin{pmatrix} \beta_1(\beta_1 l_3 + m) & \beta_4(l_2 n - l_1(\beta_4(l_3 - l_2) + m)) \\ 0 & \beta_4(\beta_4 l_2 + m)(l_2 + \beta_4(\beta_4 l_3 + m)) \end{pmatrix} \begin{pmatrix} \phi_1 \\ \phi_4 \end{pmatrix} = 0$$

Nontrivial solution to the boundary condition (17a) requires

$$\left(2l_2(l_2+l_3) - m\left(\sqrt{m^2 - 4l_2l_3} + m\right)\right) = 0$$

If $\beta_1 = \beta_4 \Leftrightarrow l_2 = l_3$, the condition for nontrivial solution is

$$A \begin{pmatrix} \psi_1^{1,4,A} \\ \psi_1^{1,4,B} \end{pmatrix} + B^{\mathrm{T}} \begin{pmatrix} \psi_2^{1,4,A} \\ \psi_2^{1,4,B} \end{pmatrix} = 0$$

There is no solution in this condition.

Denote the eigenvector corresponding to β_2 and β_3 as ϕ^2 and ϕ^3 .

$$\phi^{2} = (\beta_{2}\phi^{2,A} \ \beta_{2}\phi^{2,B} \ \beta_{2}^{2}\phi^{2,A} \ \beta_{2}^{2}\phi^{2,B} \ \cdots \ \beta_{2}^{N}\phi^{2,A} \ \beta_{2}^{N}\phi^{2,B})^{T}$$

$$\phi^{3} = (\beta_{3}\phi^{3,A} \ \beta_{3}\phi^{3,B} \ \beta_{2}^{2}\phi^{3,A} \ \beta_{2}^{2}\phi^{3,B} \ \cdots \ \beta_{3}^{N}\phi^{3,A} \ \beta_{2}^{N}\phi^{3,B})^{T}$$

The bulk recurrence relation Eq. (20) gives

$$\begin{pmatrix} l_1 + n\beta_2 + l_1\beta_2^2 & l_2 + m\beta_2 + l_3\beta_2^2 \\ 0 & 0 & 0 \end{pmatrix} \begin{pmatrix} \phi^{2,A} \\ \phi^{2,B} \end{pmatrix} = 0$$
$$\begin{pmatrix} l_1 + n\beta_3 + l_1\beta_3^2 & 0 \\ l_3 + m\beta_3 + l_2\beta_3^2 & 0 \end{pmatrix} \begin{pmatrix} \phi^{3,A} \\ \phi^{3,B} \end{pmatrix} = 0$$

Set

$$\begin{cases} \phi^{2,A} = (l_2 + m\beta_2 + l_3\beta_2^2)\phi_2\\ \phi^{2,B} = -(l_1 + n\beta_2 + l_1\beta_2^2)\phi_2\\ \phi^{3,A} = 0\\ \phi^{3,B} = \phi_3 \end{cases}$$

 $\phi_2, \phi_4 \in \mathbb{R}$. A potential solution is a linear combination of ϕ^2 and ϕ^3 .

$$\psi^{2,3} = \begin{pmatrix} \psi_1^{2,3,A} & \psi_1^{2,3,B} & \psi_2^{2,3,A} & \psi_2^{2,3,B} & \cdots & \psi_N^{2,3,A} & \psi_N^{2,3,B} \end{pmatrix}^{\mathrm{T}} \begin{pmatrix} \psi_l^{2,3,A} \\ \psi_l^{2,3,B} \end{pmatrix} = \beta_2^l \begin{pmatrix} l_2 + m\beta_2 + l_3\beta_2^2 \\ -(l_1 + n\beta_2 + l_1\beta_2^2) \end{pmatrix} \phi_2 + \beta_3^l \begin{pmatrix} 0 \\ 1 \end{pmatrix} \phi_3$$

If $\beta_2 \neq \beta_3 \Leftrightarrow l_2 \neq l_3$, the boundary condition (17b) renders

$$\begin{pmatrix} \beta_2^{N+1}(\beta_2 l_3 n - l_1 (l_2 - l_3 + \beta_2 m)) & \beta_3^{N-1}(l_2 + \beta_3 m) \\ \beta_2^{N-1}(l_3 + \beta_2 m)(l_2 + \beta_2 (\beta_2 l_3 + m)) & 0 \end{pmatrix} \begin{pmatrix} \phi_2 \\ \phi_3 \end{pmatrix} = 0$$

Nontrivial solution to the boundary condition (17b) requires

$$-\beta_2^{N-1}\beta_3^{N-1}(l_2+\beta_3m)(l_3+\beta_2m)(l_2+\beta_2(\beta_2l_3+m))=0$$

There is no solution in this condition. If $\beta_2 = \beta_3 \Leftrightarrow l_2 = l_3$, the condition for nontrivial solution is

$$B\begin{pmatrix} \psi_{N-1}^{2,3,A} \\ \psi_{2,3,B}^{2,3,B} \end{pmatrix} + A\begin{pmatrix} \psi_{N}^{2,3,A} \\ \psi_{N}^{2,3,B} \end{pmatrix} = 0.$$

There is no solution in this condition.

Case IV. $|\beta_1| < 1$, $|\beta_2| > 1$, $|\beta_3| < 1$, $|\beta_4| > 1$.

Denote the eigenvector corresponding to β_1 and β_3 as ϕ^1 and ϕ^3 , respectively.

$$\phi^{1} = (\beta_{1}\phi^{1,A} \ \beta_{1}\phi^{1,B} \ \beta_{1}^{2}\phi^{1,A} \ \beta_{1}^{2}\phi^{1,B} \ \cdots \ \beta_{1}^{N}\phi^{1,A} \ \beta_{1}^{N}\phi^{1,B})^{\mathrm{T}}$$

$$\phi^{3} = (\beta_{3}\phi^{3,A} \ \beta_{3}\phi^{3,B} \ \beta_{3}^{2}\phi^{3,A} \ \beta_{3}^{2}\phi^{3,B} \ \cdots \ \beta_{3}^{N}\phi^{3,A} \ \beta_{3}^{N}\phi^{3,B})^{\mathrm{T}}$$

The bulk recurrence relation Eq. (20) gives

$$\begin{pmatrix} l_1 + n\beta_1 + l_1\beta_1^2 & 0 \\ l_3 + m\beta_1 + l_2\beta_1^2 & 0 \end{pmatrix} \begin{pmatrix} \phi^{1,A} \\ \phi^{1,B} \end{pmatrix} = 0$$
$$\begin{pmatrix} l_1 + n\beta_3 + l_1\beta_3^2 & 0 \\ l_3 + m\beta_3 + l_2\beta_3^2 & 0 \end{pmatrix} \begin{pmatrix} \phi^{3,A} \\ \phi^{3,B} \end{pmatrix} = 0$$

Set

$$\begin{cases} \phi^{1,A} = 0 \\ \phi^{1,B} = \phi_1 \end{cases}$$
$$\begin{cases} \phi^{3,A} = 0 \\ \phi^{3,B} = \phi_3 \end{cases}$$

 $\phi_1, \phi_3 \in \mathbb{R}$. A potential solution $\psi^{1,3}$ is a linear combination of ϕ^1 and ϕ^3 .

$$\psi^{1,3} = \begin{pmatrix} \psi_1^{1,3,A} & \psi_1^{1,3,B} & \psi_2^{1,3,A} & \psi_2^{1,3,B} & \cdots & \psi_N^{1,3,A} & \psi_N^{1,3,B} \end{pmatrix}^{\mathrm{T}} \begin{pmatrix} \psi_l^{1,3,A} \\ \psi_l^{1,3,B} \end{pmatrix} = \beta_1^l \begin{pmatrix} 0 \\ 1 \end{pmatrix} \phi_1 + \beta_3^l \begin{pmatrix} 0 \\ 1 \end{pmatrix} \phi_3$$

If $\beta_1 \neq \beta_3 \Leftrightarrow m^2 \neq 4l_2l_3$, the boundary condition (17a) renders

$$\begin{pmatrix} \beta_1(\beta_1 l_3 + m) & \beta_3(\beta_3 l_3 + m) \\ 0 & 0 \end{pmatrix} \begin{pmatrix} \phi_1 \\ \phi_3 \end{pmatrix} = 0 \tag{A16}$$

(A16) always has nontrivial solutions to ϕ_1 and ϕ_3 . Therefore, there always exist boundary states satisfying the boundary condition (17a).

If $m^2 = 4l_2l_3$, $\beta_1 = \beta_3 = \frac{-m}{2l_3}$, the condition for nontrivial solution is

$$A \begin{pmatrix} \psi_1^{1,3,A} \\ \psi_1^{1,3,B} \end{pmatrix} + B^{\mathrm{T}} \begin{pmatrix} \psi_2^{1,3,A} \\ \psi_2^{1,3,B} \end{pmatrix} = 0$$

There is no solution in this condition. Denote the eigenvector corresponding to β_2 and β_4 as ϕ^2 and ϕ^4 , respectively.

$$\phi^{2} = (\beta_{2}\phi^{2,A} \ \beta_{2}\phi^{2,B} \ \beta_{2}^{2}\phi^{2,A} \ \beta_{2}^{2}\phi^{2,B} \ \cdots \ \beta_{2}^{N}\phi^{2,A} \ \beta_{2}^{N}\phi^{2,B})^{T}$$

$$\phi^{4} = (\beta_{4}\phi^{4,A} \ \beta_{4}\phi^{4,B} \ \beta_{4}^{2}\phi^{4,A} \ \beta_{4}^{2}\phi^{4,B} \ \cdots \ \beta_{4}^{N}\phi^{4,A} \ \beta_{4}^{N}\phi^{4,B})^{T}$$

The bulk recurrence relation Eq. (20) gives

$$\begin{pmatrix} l_1 + n\beta_j + l_1\beta_j^2 & l_2 + m\beta_j + l_3\beta_j^2 \\ 0 & 0 \end{pmatrix} \begin{pmatrix} \phi^{j,A} \\ \phi^{j,B} \end{pmatrix} = 0, \quad j = 2, 4$$

Set

$$\phi^{j,A} = (l_2 + m\beta_j + l_3\beta_j^2)\phi_j$$

$$\phi^{j,B} = -(l_1 + n\beta_j + l_1\beta_j^2)\phi_j$$

 $\phi_i \in \mathbb{R}$. A potential solution $\psi^{2,4}$ is a linear combination of ϕ^2 and ϕ^4 .

$$\psi^{2,4} = \left(\psi_1^{2,4,A} \ \psi_1^{2,4,B} \ \psi_2^{2,4,A} \ \psi_2^{2,4,B} \ \cdots \ \psi_N^{2,4,A} \ \psi_N^{2,4,B}\right)^{\mathrm{T}}$$

$$\begin{pmatrix} \psi_l^{2,4,A} \\ \psi_l^{2,4,B} \end{pmatrix} = \beta_2^l \begin{pmatrix} l_2 + m\beta_2 + l_3\beta_2^2 \\ -(l_1 + n\beta_2 + l_1\beta_2^2) \end{pmatrix} \phi_2 + \beta_4^l \begin{pmatrix} l_2 + m\beta_4 + l_3\beta_4^2 \\ -(l_1 + n\beta_4 + l_1\beta_4^2) \end{pmatrix} \phi_4$$

If $\beta_2 \neq \beta_4 \Leftrightarrow m^2 \neq 4l_1l_2$, the boundary condition (17b) renders

$$(l_2 - l_3)(n(l_2 + l_3) - 2l_1m) = 0$$

 $l_2=l_3$ renders $|\beta_2|=|\beta_3|=1$ or $|\beta_2||\beta_3|=1$, which is out of consideration. If $m^2=4l_2l_3$, $\beta_2=\beta_4=\frac{-m}{2l_2}$, the condition for nontrivial solution is

$$B\begin{pmatrix} \psi_{N-1}^{2,4,A} \\ \psi_{N-1}^{2,4,B} \end{pmatrix} + A\begin{pmatrix} \psi_{N}^{2,4,A} \\ \psi_{N}^{2,4,B} \end{pmatrix} = 0$$

which renders

$$\begin{cases} l_2 = l_3 \\ 2|l_1| = |n| \\ |m| = 2|l_2| \end{cases}$$

In this case, $|\beta_2| = |\beta_4| = 1$, which means that the assumption is wrong. There is no solution.

Case I $|\beta_1| > 1$, $|\beta_2| < 1$, $|\beta_3| > 1$, $|\beta_4| < 1$ and Case IV $|\beta_1| < 1$, $|\beta_2| > 1$, $|\beta_3| < 1$, $|\beta_4| > 1$ can be summarized and combined into the condition $|m| < |l_2 + l_3|$. In summary, we find a class of K-matrices possessing zero modes, as shown in Table I.